frontiers in Built Environment

TYPE Original Research
PUBLISHED 20 March 2026
DOI 10.3389/fbuil.2026.1783466

Check for updates

OPEN ACCESS

EDITED BY
Giuseppina Emma Puglisi,
Polytechnic University of Turin, Italy

REVIEWED BY
Yicheng Wang,
Polytechnic University of Turin, Italy
Hadjira Sakhri,
University of Biskra, Algeria

*CORRESPONDENCE
Gizem Izmir Tunahan,
gizem.izmirtunahan@deu.edu.tr

RECEIVED 08 January 2026
REVISED 06 February 2026
ACCEPTED 12 February 2026
PUBLISHED 20 March 2026

CITATION
Izmir Tunahan G and Özer Yaman G (2026) Climate-adaptive passive design for sustainable libraries: simulation and machine learning-based multi-objective optimisation of comfort, energy, and environmental performance.
Front. Built Environ. 12:1783466.
doi: 10.3389/fbuil.2026.1783466

COPYRIGHT
© 2026 Izmir Tunahan and Özer Yaman. This is an open-access article distributed under the terms of the Creative Commons Attribution License (CC BY). The use, distribution or reproduction in other forums is permitted, provided the original author(s) and the copyright owner(s) are credited and that the original publication in this journal is cited, in accordance with accepted academic practice. No use, distribution or reproduction is permitted which does not comply with these terms.

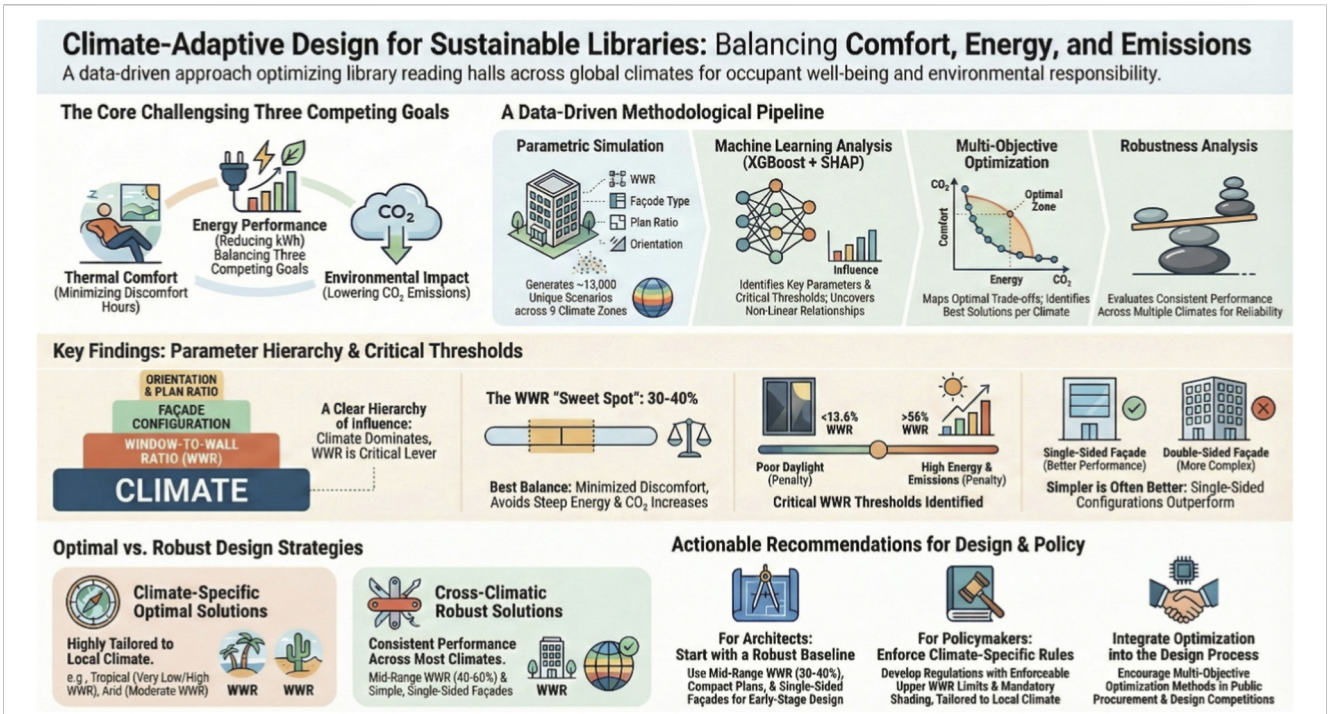
Climate-adaptive passive design for sustainable libraries: simulation and machine learning-based multi-objective optimisation of comfort, energy, and environmental performance

Gizem Izmir Tunahan[1]* and Gonca Özer Yaman[2,3]

[1]Department of Architecture, Faculty of Architecture, Dokuz Eylul University, İzmir, Türkiye, [2]Department of Architecture, Faculty of Engineering and Architecture, Bingöl University, Bingöl, Türkiye, [3]Centre for Energy, Environment, and Natural Disasters, Bingöl University, Bingöl, Türkiye

Library reading halls are critical environments where long-term user comfort must be balanced with stringent energy and carbon reduction goals. Passive design parameters-such as aspect ratio, façade configuration, window-to-wall ratio (WWR), and orientation-play a key role in shaping these outcomes, yet comprehensive cross-climatic evaluations remain limited. This study evaluates nearly 13,000 simulation scenarios across nine Köppen climate zones, varying plan geometry, façade configuration, WWR (10%–90%), and orientation. The methodological framework combines statistical effect analysis with explainable machine learning (XGBoost-SHAP) to identify dominant drivers, non-linear interactions, and critical thresholds. Multi-objective Pareto-based optimisation and robustness analysis are then employed to derive climate-responsive design strategies balancing thermal discomfort hours, total site energy use, and CO_2 emissions. Results show that climate and WWR dominate performance, with façade configuration secondary and orientation and plan ratio context-dependent. Optimal outcomes clustered around mid-range WWR values (30%–40%), while very low and high ratios imposed performance penalties. Compact plans with single-sided façades generally favoured energy and CO_2 reduction, whereas elongated plans with double-sided façades improved comfort. Optimisation confirmed the absence of a universal optimum but identified mid-range archetypes (WWR 40%–60%, single façades) that offer superior resilience against climatic uncertainty. The study provides actionable, climate-sensitive thresholds to guide early-stage design. For practice, it offers actionable rules for architects, while for policy, it supports climate-specific guidelines, such as enforceable upper WWR limits, mandatory shading in high-glazing scenarios, and the integration of optimisation methods into procurement processes. Beyond libraries, the framework demonstrates a transferable pipeline for climate-adaptive, low-carbon building design that aligns with international sustainability goals. While visual comfort is implicitly addressed through energy penalties for insufficient daylight, future research should extend this framework by integrating detailed glare and visual quality metrics to fully reconcile thermal resilience with user-centric lighting needs.

KEYWORDS
building simulation, climate-adaptive design, energy performance, multi-objective optimisation, passive design, thermal comfort, window-to-wall ratio (WWR), XGBoost



GRAPHICAL ABSTRACT

1 Introduction

Globally, buildings are responsible for nearly one-third of total energy use and around 37% of energy-related carbon emissions, positioning the built environment at the centre of climate change mitigation strategies (Yaman, 2025; Du et al., 2025). Within this sector, heating, cooling and lighting represent the dominant end-uses, highlighting the significant potential of design interventions to reduce demand (Hu et al., 2023; Aflaki et al., 2023). Beyond energy considerations, however, the concept of indoor environmental quality (IEQ) has emerged as a critical determinant of building performance, encompassing not only operational efficiency but also the health, productivity and wellbeing of occupants (Thneibat, 2024; Baba et al., 2024).

IEQ is a multidimensional concept encompassing indoor air quality, thermal, visual, and acoustic comfort, as well as ergonomics and safety (Baba et al., 2024). Research shows that IEQ conditions directly impact learning, attention, and cognitive performance (Pellerin and Candas, 2003; Banbury and Berry, 2005). For example, even a 1 °C temperature deviation can significantly reduce user comfort and create a negative impact equivalent to a 2–3 dB increase in noise (Thneibat, 2024). Similarly, insufficient daylight disrupts students' circadian rhythms, which can adversely affect their attention and achievement (Baba et al., 2024).

Educational buildings and libraries hold a special position in IEQ discussions. These buildings accommodate long-term intensive use, different user profiles, and learning-focused activities (Thneibat, 2024; Tunahan et al., 2022). Research has shown that HVAC systems and lighting account for 70%–80% of total energy consumption in libraries, yet thermal and visual comfort often fail to reach adequate levels. Furthermore, it is emphasised that temperature and humidity in tropical regions critically affect the preservation of book collections (Aflaki et al., 2023). Therefore, a delicate balance must be struck in educational buildings between reducing energy consumption and increasing user comfort.

Studies evaluating IEQ and energy performance in the literature are shaped around two main approaches. The first trend involves methodological approaches to measuring IEQ. Traditionally, sensor-based measurements provide objective data; however, these data have limitations in reflecting the user experience (Baba et al., 2024). For this reason, user feedback-based methods, such as Post-Occupancy Evaluation (POE), have become increasingly widespread in recent years (Thneibat, 2024). Indeed, a POE study conducted in Palestine showed that students' perceptions of thermal, acoustic, and visual comfort in classrooms revealed problems that could not be detected by technical measurements alone (Baba et al., 2024). Similarly, large-scale text mining analyses highlight dissatisfaction with different IEQ parameters, demonstrating the importance of new data-driven methods (Thneibat, 2024).

The second trend involves research examining the effects of passive design parameters on energy consumption and user comfort. Passive strategies have historically been used in hot climates to ensure indoor habitability without the need for mechanical systems (Hu et al., 2023). Today, parameters such as the window-to-wall ratio (WWR), façade configuration, orientation, and building geometry are among the most critical design variables for both energy consumption and comfort (Sayadi et al., 2021; Tawfeeq and Qaradaghi, 2024). Research has shown that optimal WWR values vary significantly depending on climatic conditions, and incorrect choices can increase total energy consumption by up to 25% (Goia, 2016). Simulation studies conducted in various climate zones,

including Turkey, Iran, and Sweden, have demonstrated that WWR is a crucial parameter for determining heating, cooling, and lighting loads (Sayadi et al., 2021). Similarly, research conducted in Mediterranean climates has shown that reducing WWR by 20% can lead to a 15% reduction in energy usage (Tawfeeq and Qaradaghi, 2024).

Building geometry, orientation, and façade characteristics are also decisive factors in this context. For example, a study conducted on industrial buildings in Turkey demonstrated that different geometric shapes significantly affected energy performance across five distinct climate zones, and that optimal solutions could be achieved through artificial intelligence-supported optimisation (Yaman, 2025). Similarly, a study of high-rise offices in China's hot-summer, temperate-winter region found that energy consumption and daylight comfort could be optimised simultaneously by integrating artificial intelligence (ANN, SVM, XGBoost) and genetic algorithms (Xie et al., 2025). In educational buildings, a study conducted at Tianjin University showed that optimising façade parameters using genetic algorithms resulted in improvements of up to 63% in cooling loads and 95% in heating loads (Du et al., 2025).

Passive design parameters interact strongly with climate; the same intervention can produce different directions and magnitudes of effects in tropical, arid, or continental contexts. For example, the impact of the window-to-wall ratio (WWR) on energy use and comfort varies meaningfully with climate and orientation, and identical WWR values can lead to opposite outcomes across climates (Goia, 2016; Ochoa et al., 2012a). Solar geometry and shading must be considered in conjunction with the architectural design, particularly in hot-summer climates, where appropriate shading can significantly reduce cooling loads. However, the most effective shading strategy varies by climate (Tzempelikos and Athienitis, 2007). Envelope and glazing configurations, as well as insulation levels, are highly dependent on climate. Heating demand predominates at temperate to cold temperatures, whereas cooling and humidity control requirements are more pronounced in hot, humid regions (Ochoa et al., 2012a). Orientation and massing (aspect ratio, surface-to-volume relationships) yield different "best" solutions for both heating/cooling loads and daylight performance, depending on the climate (Ratti et al., 2005). Consequently, findings derived from a single climate have limited generalisability; comparative studies representing multiple climate classes are necessary to derive transferable design rules (Kottek et al., 2006; Peel et al., 2007).

Recent research has examined passive design strategies across diverse climates. For example, Aflaki et al. (2023) evaluated indoor environmental quality in tropical libraries, highlighting the persistent trade-offs between comfort and energy efficiency, although their study was limited to a single climatic context. Yaman, (2025) optimised passive parameters for industrial buildings in arid regions using ANN and PSO, but the findings remain typology-specific and not transferable to educational spaces. Tawfeeq and Qaradaghi (2024) investigated WWR optimisation in hot-summer Mediterranean climates, yet their scope did not extend to multi-objective comfort–energy–carbon trade-offs. In East Asia, Xie et al. (2025) applied machine learning and genetic algorithms to optimise high-rise office façades in China's hot-summer/warm-winter zone, while Du et al. (2025) developed a renovation framework for educational buildings in Tianjin. However, both studies remained limited to a single region. Goia, (2016) and Sayadi et al. (2021) demonstrated the climatic sensitivity of WWR thresholds in European and Middle Eastern contexts, respectively, but did not address robustness across multiple climates. More recent contributions also reflect growing interest in educational buildings: Baba et al. (2024) reported user-perceived IEQ problems in Palestinian schools through POE, and Thneibat (2024) applied structural equation modelling to explore post-COVID comfort dynamics in Jordanian classrooms, both underscoring the gap between measured and experienced comfort. In North America, Yeom et al. (Yeom et al., 2020) demonstrated that office window size strongly influences both task performance and energy demand, while Ascione et al. (2017a) highlighted the potential of ANN-based prediction for retrofit scenarios; however, neither study addressed library typologies. Similarly, Hamdy et al. (2011) explored multi-objective optimisation for dwellings in Finland, but their findings remain climate- and use-specific.

Despite valuable contributions, the current literature remains constrained in several respects. The first limitation is that most studies continue to focus on residential or office buildings, whereas libraries and educational facilities with their distinctive user profiles, long-stay occupancy, and learning-oriented functions remain underexplored. The second limitation is that research is frequently confined to single climatic contexts, which restricts the transferability of findings and weakens the universal validity of design thresholds. The third limitation is that many investigations emphasise a single performance indicator, such as energy use or daylighting, rather than addressing the multidimensional nature of indoor environmental quality, parameter interactions, and comfort–energy–carbon relationships. The fourth limitation is that while some recent works employ advanced optimisation or AI techniques, these approaches are rarely combined with interpretable machine learning and robustness testing. Addressing these limitations requires a large-scale, cross-climatic, and library-specific framework that unites parametric simulation, explainable ML, and multi-objective optimisation into a coherent methodology.

This study undertakes a large-scale simulation analysis of library reading halls across 9 Köppen climate zones, generating approximately 13,000 scenarios. The investigation systematically evaluates four passive design parameters, window-to-wall ratio (WWR), façade configuration, orientation, and geometric proportions and examines their combined influence on thermal comfort, site energy demand, and CO_2 emissions. Statistical effect analysis was used to quantify the influence of parameters, while machine learning (XGBoost) with SHAP interpretation revealed variable importance, non-linear interactions, and critical thresholds. Multi-objective optimisation with Pareto fronts was then applied to establish climate-adaptive design solutions and assess robustness across climates.

While the primary optimisation objectives are thermal comfort, site energy demand, and CO_2 emissions, the study implicitly accounts for daylight availability through the daylight-linked

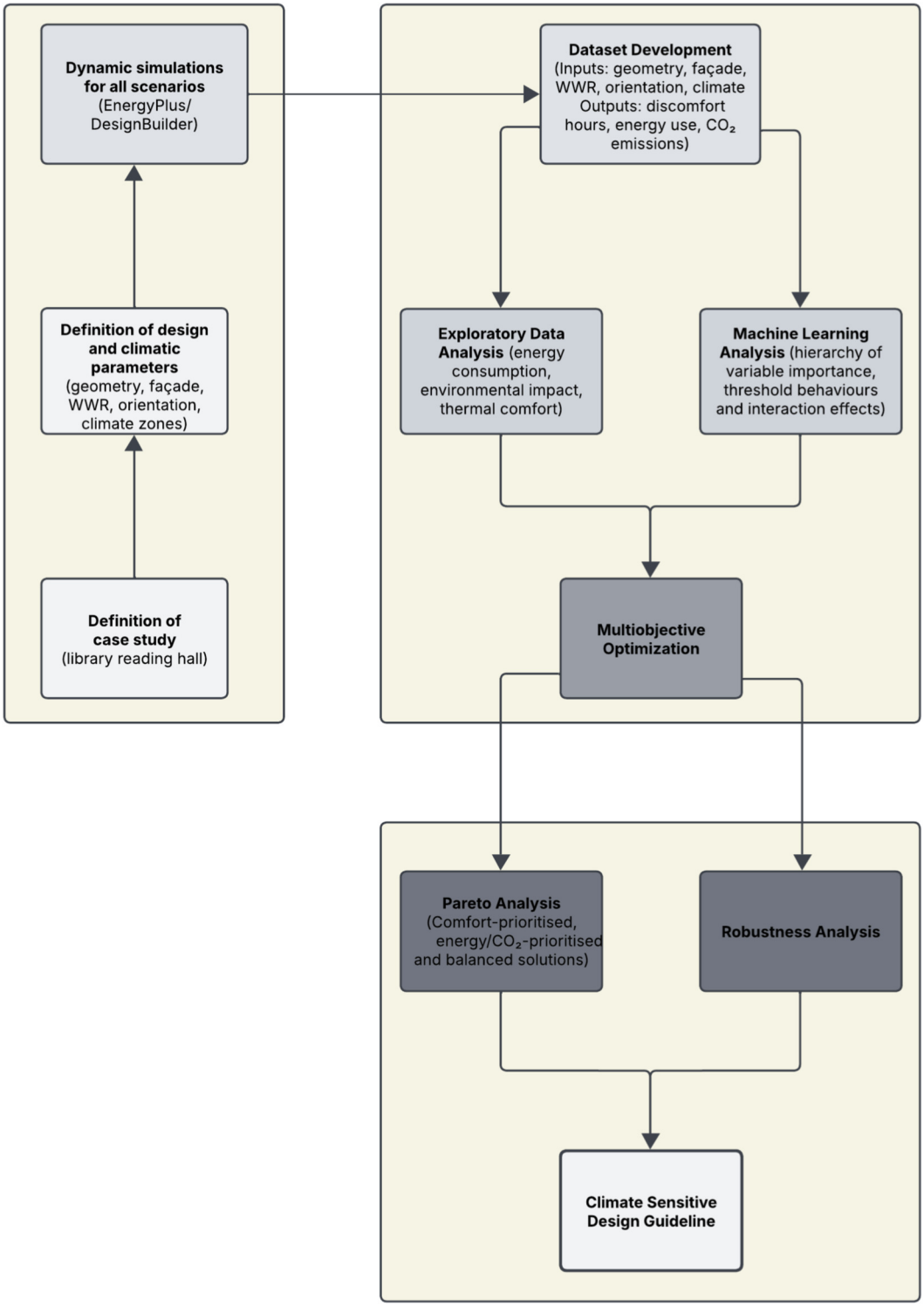


FIGURE 1
Overview of the methodological workflow.

lighting control protocols implemented in the simulation. Thus, scenarios with insufficient daylight (e.g., very low window-to-wall ratio, WWR) are penalised with higher lighting energy demands, ensuring that energy-efficient solutions do not compromise basic illuminance requirements. Consequently, visual comfort is addressed primarily through its impact on energy balance, while specific glare metrics remain a priority for future detailed design stages.

2 Methodology

2.1 Methodological framework

The research employed a multi-stage methodological framework that integrated building performance simulation, data-driven modelling, and optimisation. The workflow was designed to ensure that the study not only quantified the direct effects of passive design parameters but also extracted underlying interactions, thresholds, and trade-offs across diverse climate contexts.

As illustrated schematically in Figure 1, the process began with systematically varying independent design variables (geometry, façade configuration, window-to-wall ratio, orientation) across 9 Köppen–Geiger climate zones. This parametric modelling generated a comprehensive dataset of approximately 13,000 scenarios using DesignBuilder with the EnergyPlus engine. The dataset was first examined through exploratory data analysis (EDA) to capture broad distributions and median trends by climate and design variable. Subsequently, machine learning regression models (XGBoost) were trained to predict key performance outcomes, including discomfort hours, energy use, and CO_2 emissions, and were interpreted through SHAP (Shapley Additive exPlanations) values. This step provided parameter importance rankings, non-linear interaction effects, and identification of critical design thresholds. Finally, multi-objective optimisation was applied using Pareto front analysis, deriving climate-sensitive solutions that balanced comfort, energy demand, and carbon emissions. Robustness testing across climates confirmed the stability of recommendations. This staged approach provided a structured pathway from raw simulation data to interpretable machine learning insights and optimised design strategies, bridging the gap between parameter testing and actionable climate-adaptive guidance.

2.2 Case study definition and simulation setup

The case study focused on library reading halls, a building typology where students spend prolonged periods engaged in concentrated tasks. These spaces are susceptible to issues related to indoor environmental quality, as thermal comfort directly impacts user productivity, while energy efficiency remains crucial for sustainable operation. Unlike residential or office buildings, libraries present unique challenges since occupant well-being and collection preservation depend on carefully controlled environmental conditions.

Their climatic and cultural relevance also justifies the choice of library reading halls. In tropical regions, stable temperature and humidity are critical not only for user comfort but also for preserving books and archival materials (Silva and Henriques, 2015; Silva and Henriques, 2014). In arid and Mediterranean climates, solar gains and glare create persistent risks of overheating and visual discomfort (Ascione et al., 2017a), particularly in regions where extended afternoon and evening study patterns are typical (Applegate, 2009). In temperate and continental contexts, heating demand typically dominates, and the performance of the envelope becomes a decisive factor (Goia, 2016). Beyond climatic constraints, cultural patterns also shape library use: in some regions, libraries primarily function as student study spaces with extended periods of sedentary activity, while in others, they serve as community hubs or archival repositories with intermittent but high-density occupancy. Expectations of quiet, lighting quality, and thermal tolerance also vary across cultures, influencing how users interact with the space and adapt to environmental conditions (Frontczak and Wargocki, 2011; Izmir Tunahan et al., 2022). These combined climatic, regional, and cultural factors make library reading halls an especially sensitive and globally relevant typology for climate-adaptive passive design. Therefore, the simulation campaign was organised around a set of controlled parameters to systematically examine the interaction between passive design strategies and diverse climatic contexts. The parameter space was deliberately limited to four variables: window-to-wall ratio (WWR), orientation, plan ratio, and façade configuration, because these constitute the primary geometric and envelope-related drivers of daylight and thermal performance at the early design stage. Other passive measures, such as shading devices, glazing types, insulation levels, and natural ventilation, were excluded to preserve the tractability of the simulation set and to allow meaningful incorporation in subsequent phases once fundamental geometric sensitivities are established. This stepwise approach follows established practice in parametric studies, where geometric parameters are isolated first to reveal baseline performance drivers before expanding to material and operational variables (Compagnon, 2004; AlAnzi et al., 2009; Goia, 2016; Sayadi et al., 2021).

- Architectural details: The case-study model was defined as a standardised library reading hall to enable controlled comparison across climates. The net floor area was fixed at 60 m^2, accommodating 30 occupants (approximately 2.0 m^2 per person) with a clear height of 3.5 m, resulting in a total volume of 210 m^3. This 60 m^2 geometry should be interpreted not as a standalone building, but as a representative 'thermal module' or 'unit cell' commonly found in larger library reading halls. By analysing this fundamental unit, the results can be extrapolated to larger open-plan layouts composed of similar repeating peripheral zones. These values were defined in accordance with international library design guidelines (IFLA (Latimer and Niegaard, 2007)) and indoor air quality standards (ASHRAE Standard 62.1 (ANSI and ASHRAE, 2022)).

Three plan ratios (1:1, 1:1.5, and 1:2) were adopted as simplified geometric archetypes to represent the progression from compact to elongated layouts in institutional reading halls. This range was sufficient to capture the performance shifts associated with increasing room depth, which directly affects the surface-to-volume ratio, daylight penetration, and thermal response. The significance of plan geometry as a determinant of building performance is well established: Compagnon, (2004) demonstrated that greater room depth reduces daylight availability in the occupied zone; AlAnzi et al. (2009) showed that elongated forms increase thermal loads in hot-arid climates, and Goia, (2016), together with Sayadi et al. (2021), confirmed that

façade geometry and window-to-wall ratio substantially influence both daylight and energy demand across diverse climatic contexts. More extreme ratios (e.g., 1:3) were excluded, as such deep-plan configurations are rare in library reading halls and often create impractical daylighting and visual conditions. The chosen range, therefore, strikes a balance between functional relevance and analytical tractability, ensuring meaningful yet manageable cross-climatic comparisons.

Two façade configurations, single-sided glazing and double-sided glazing, were considered. These were selected as archetypal strategies commonly employed in reading hall design to capture contrasting daylighting and ventilation logics. According to guidelines by the Chartered Institution of Building Services Engineers (CIBSE) (CIBSE, 2015) and the Illuminating Engineering Society of North America (IESNA) (IESNA, 2012), single-sided glazing, often found in compact or site-constrained layouts, typically restricts daylight penetration to a depth of about 6–7 m and limits opportunities for cross-ventilation (Nicol and Humphreys, 2002). By contrast, double-sided glazing, more characteristic of elongated layouts, allows daylight to penetrate deeper into the occupied zone and enables effective cross-ventilation (Compagnon, 2004), though at the expense of increased solar exposure and potentially higher cooling loads (Tregenza and Wilson, 2011). Including both variants allowed the study to capture these realistic performance trade-offs while avoiding the overgeneralisation of representing all possible library typologies.

These plan ratios and façade configurations were not intended to replicate specific regional case studies, but rather to serve as simplified archetypes that capture the key performance sensitivities of reading halls in terms of daylight penetration, surface-to-volume ratio, and thermal response (Compagnon, 2004; AlAnzi et al., 2009; Goia, 2016; Sayadi et al., 2021). Fixing these archetypes across climates enabled controlled comparison of passive design parameters under consistent boundary conditions, ensuring that the results can be interpreted as comparative thresholds and sensitivities rather than as universal prescriptions.

The envelope was represented by a standardised brick–insulation–concrete assembly with a U-value of 0.35 W/m^{2}K, and glazing was defined as clear double-glazing (3-13–3 mm), following benchmark construction types commonly used in comparative simulation studies (Goia, 2016). This combination of guideline-based thresholds and standardised baselines ensured that the architectural model was consistent, reproducible, and suitable for cross-climatic analysis.

- Geometry: The plan variations were derived by maintaining a constant total floor area, based on the recommended minimum square metres per person for library reading halls. This ensured that each configuration provided an equivalent usable space per occupant, thereby isolating the effects of geometry rather than differences in size. Within this constraint, three plan ratios were defined: 1:1 (square), 1:1.5 (moderately elongated rectangle), and 1:2 (elongated rectangle) to represent standard institutional layouts (Figure 2). These variations allowed the analysis of how shape alone influences surface-to-volume ratio, daylight penetration depth, and thermal behaviour, while maintaining comparability across cases.
- Façade configuration: Two alternatives were tested: single-sided glazing, representing the baseline with limited daylight penetration and ventilation potential, and double-sided glazing, which enables cross-ventilation and improves the uniformity of daylight distribution (Figure 2).
- Window-to-wall ratio (WWR): Glazing proportions ranged from 10% to 100% in 10% increments, spanning from under-glazed to fully glazed conditions.
- Orientation: The models were rotated between 0° and 360° at 15° intervals, allowing for the assessment of solar exposure across seasonal and climatic variations.

The present study intentionally focused on four primary passive design parameters-WWR, façade configuration, orientation, and plan ratio-that are defined at early design stages and directly constrain the building's geometric and envelope potential. Other passive measures, such as external shading devices, glazing properties, insulation levels, and natural ventilation strategies, were excluded to limit model dimensionality and ensure tractable cross-climatic comparison across a large parametric design space.

Climate scenarios: Passive design parameters are strongly influenced by climatic conditions, with the same intervention producing different directions and magnitudes of effect in tropical, arid, or continental regions, owing to variations in dominant heating and cooling loads, solar geometry, humidity regimes, and diurnal temperature ranges. Consequently, results derived from a single climate are of limited generalisability. In this study, cities representing nine distinct Köppen–Geiger classes with global geographic coverage were selected to ensure that the findings could be meaningfully compared and transferred across contexts. Nine representative cities spanning distinct Köppen–Geiger classes were chosen to ensure diversity across tropical, arid, and temperate contexts: Singapore (Af, equatorial rainforest), Goa, India (Aw, tropical savanna), Madinah, Saudi Arabia (BWh, hot desert), Turpan, China (BWk, cold desert), Phoenix, United States (BSh, hot semi-arid), İzmir, Turkey (Csa, Mediterranean hot-summer), London, UK (Cfb, marine oceanic), Shanghai, China (Cfa, humid subtropical), and Ann Arbor, United States (Dfa, humid continental). This set of locations captured extreme and moderate climatic conditions, enabling the evaluation of passive design strategies across a broad environmental spectrum. The monthly mean temperature profiles in Figure 3 visually demonstrate the climatic diversity underpinning the study's climate-specific analyses. This comprehensive set of locations spans a broad spectrum of climates, ranging from extreme to temperate, enabling a comparative evaluation of passive design strategies under varying environmental conditions. The selected cities are not treated as geographic case studies, but as climatic proxies representing distinct Köppen–Geiger climate classes. Their role is to provide standardised boundary conditions for climate-class-level comparison, rather than to reflect site-specific urban or cultural characteristics.

Figure 3 also highlights pronounced differences in seasonal amplitude and peak summer temperatures across climates, which directly condition the relative dominance of heating versus cooling demands and, consequently, the effectiveness of passive design

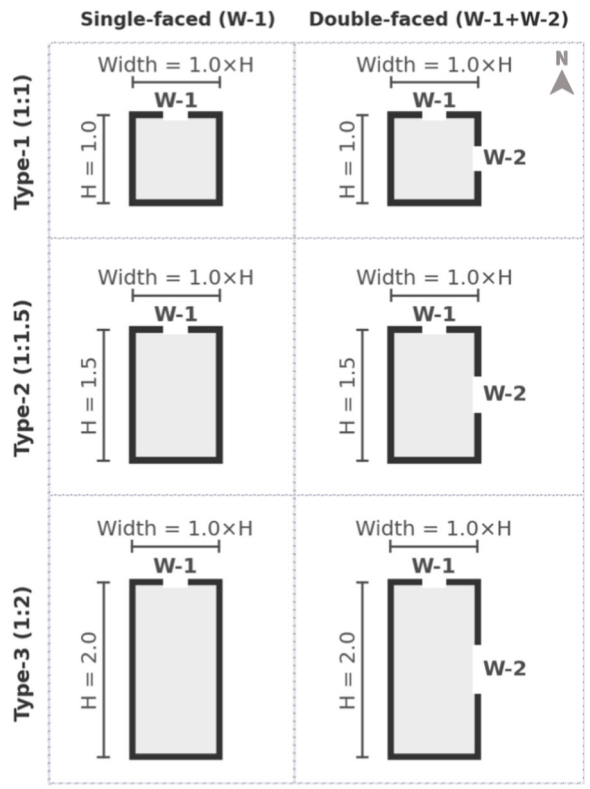


FIGURE 2
Plan-ratio typologies and façade configurations tested in the parametric study.

strategies evaluated in later sections. This figure, therefore, provides the climatic context for interpreting the subsequent energy, comfort, and optimisation results.

- Standards-based capacity and geometric normalisation: International and national guidelines for library reading rooms recommend approximately 2–2.5 m^2 of net area per user and a minimum room area of 40–60 m^2 (Department for Education and Skills, 2004). The IFLA guideline advises a minimum clear height of 3.0 m, preferably 3.5–4.0 m, for public reading spaces (Latimer and Niegaard, 2007). For ventilation, ASHRAE 62.1 (ANSI and ASHRAE, 2022) specifies 8–10 L/s of outdoor air per person, which can be converted to an air-changes-per-hour (ACH) target for a given room volume (ANSI and ASHRAE, 2022). Based on these thresholds, all plan types in this study were standardised to 30 occupants and 60 m^2 of net floor area (approximately 2.0 m^2 per person). The storey height was fixed at 3.5 m, yielding a room volume of 210 m^3. At this occupancy, 8–10 L/s·person corresponds to a total outdoor-air flow of 240–300 L/s, i.e., ACH ≈4.1–5.1 h^{-1} for a 210 m^3 space meeting the commonly used ≥3 ACH benchmark (ANSI and ASHRAE, 2022). This normalisation satisfies the minimum area/height requirements and equalises boundary conditions across climates. To preserve comparability, geometry was varied only through the plan ratio (Type-1: 1:1; Type-2: 1:1.5; Type-3: 1:2) and façade configuration (single/double), while net floor area (60 m^2) and room volume (210 m^3) were held constant in all variants. Consequently, observed performance differences can be attributed to passive design variables, such as WWR, orientation, façade type, and plan ratio, rather than to changes in size or occupancy density. The schematics of the plan-ratio typologies and façade configurations used in the parametric study are presented in Figure 2.
- User behaviour: Occupancy schedules, clothing insulation levels, and metabolic rates were defined according to international comfort and indoor environment standards such as ASHRAE Standard 55 (ASHRAE, 2020a) and ISO 7730 (ISO, 2005). Standardised occupancy and metabolic profiles were deliberately adopted to isolate the impact of passive design parameters from the noise of behavioural variability. While real-world library usage is stochastic, using fixed standard profiles ensures that the observed performance shifts are attributable solely to geometric and climatic factors, providing a consistent baseline for cross-climatic comparison.

The adaptive comfort literature has also shown that user behaviour is highly context-dependent, with responses varying across regions and cultures (de Dear and Brager, 1998; Nicol and Humphreys, 2002). Therefore, the limitations of using uniform assumptions are acknowledged, and future research will extend the analysis by calibrating it against monitored data from representative library buildings across different regions to capture behavioural diversity better. This study did not conduct sensitivity analyses of alternative behavioural profiles, but such analyses are recommended as an important direction for future work.

For all simulations, standardised occupant-related assumptions were adopted, including a metabolic rate of 0.9 met, seasonal clothing insulation values (0.50 clo for summer and 1.00 clo for winter), and fixed occupancy schedules, consistent with DesignBuilder/EnergyPlus 'All Clothing' profiles and international comfort standards. These parameters were held constant across all climate zones to ensure controlled cross-climate comparability of passive design sensitivities and to isolate the effects of climate and envelope-related design variables.

All scenarios were simulated using DesignBuilder (EnergyPlus v9.4 engine), a validated dynamic building performance modelling tool that integrates thermal, daylighting, and energy calculations. The framework relied on EnergyPlus as the underlying simulation engine, which has been extensively benchmarked across diverse building types and climatic contexts (Crawley et al., 2008) (Tian et al., 2018). The archetypal library models developed in this study were not empirically calibrated against monitored buildings; instead, standardised operational, thermal, and envelope assumptions were applied to ensure comparability across cases. Accordingly, the results are interpreted as comparative thresholds and sensitivities under controlled assumptions rather than absolute predictions for any single library. These assumptions included occupancy schedules, clothing insulation levels, heating and cooling setpoints, lighting power density, plug loads, and envelope constructions, as summarised in Table 1. A linear dimming control strategy was implemented to ensure a realistic trade-off between solar gain and daylight utilisation. This mechanism automatically adjusts artificial lighting based on daylight

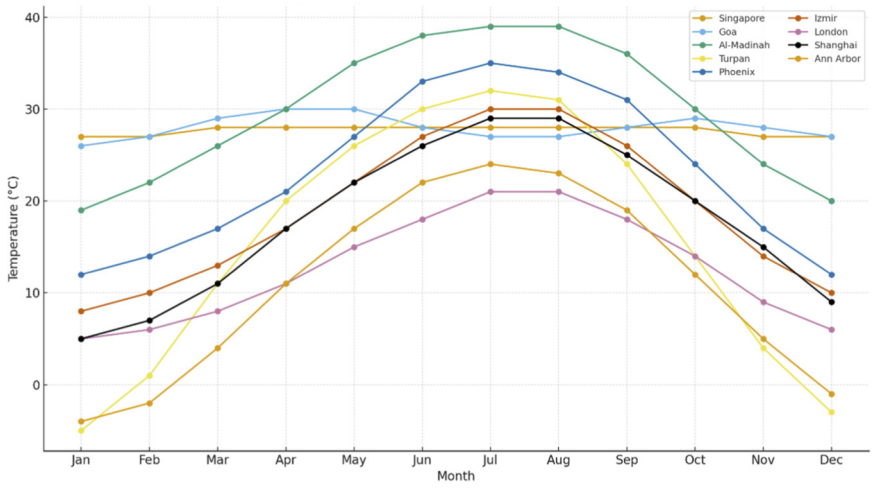


FIGURE 3
Monthly average temperature profiles (°C) for the nine case cities.

availability, meaning that the 'Total Site Energy' metric captures not only HVAC loads but also the energy penalty associated with designs with poor daylight penetration.

2.3 Dataset development

The systematic variation of geometry, façade configuration, WWR, orientation, and climate zone produced a comprehensive dataset of various scenarios. Each simulation represented a unique combination of input parameters and yielded corresponding performance outputs. As summarised in Table 2, the dataset comprised independent variables (plan ratio, façade configuration, WWR, orientation, climate) and dependent variables (thermal comfort, energy use, CO_2 emissions). It was structured to support statistical analysis and machine learning by combining categorical and continuous parameters. This structure enabled the detection of non-linear interactions, identification of critical thresholds, and development of climate-sensitive optimisation strategies.

2.4 Validation and generalisability

The simulation campaign was conducted in DesignBuilder using the EnergyPlus v9.4 engine, one of the most extensively validated building performance simulation tools. EnergyPlus has been widely verified using standardised comparative test procedures such as ANSI/ASHRAE Standard 140 (BESTEST), and published BESTEST reports for EnergyPlus support confidence in its underlying heat-balance algorithms for comparative analyses (ASHRAE, 2020b; Henninger and Witte, 2004). In addition, empirical validation studies have compared EnergyPlus outputs against monitored data from controlled test facilities, and calibration/validation case studies have also been reported for institutional buildings, including a naturally ventilated library, with studies reporting generally good agreement at the zone-load level while noting larger discrepancies at the system/plant level (Som and Gregory, 2011; Coakley et al., 2012). EnergyPlus has been benchmarked against empirical datasets for thermal comfort and energy use across a wide range of building types and climates (Crawley et al., 2008; Hopfe, 2009), providing confidence in the reliability of its underlying physics and algorithms.

The models in this study were not calibrated against field data from individual library case studies in each climate zone. Instead, operational schedules, occupancy profiles, and envelope characteristics were standardised in line with international standards, including ASHRAE 55 (ASHRAE, 2020a), ISO 7730 (ISO, 2005), ASHRAE 62.1 (ANSI and ASHRAE, 2022), and IFLA (Latimer and Niegaard, 2007). This deliberate standardisation ensured that performance differences could be attributed to the passive design parameters under study rather than to region-specific operational noise. The resulting framework, therefore, enabled reproducible, controlled comparison of design sensitivities across nine distinct climatic contexts and is consistent with prior cross-climatic simulation studies that employed archetypal models to isolate geometric and envelope effects (AlAnzi et al., 2009; Goia, 2016).

The modelling strategy was not designed to reproduce regional archetypes but to isolate the relative influence of key passive parameters, window-to-wall ratio, plan ratio, orientation, and façade configuration, under consistent boundary conditions. These parameters were selected because they represent the primary passive design drivers influencing daylight distribution, thermal loads, and comfort in reading halls, thereby providing the most direct insights into cross-climatic performance sensitivities. Accordingly, the results are interpreted as comparative thresholds and parameter hierarchies, including the proposed 30%–40% WWR "sweet spot" as a comparative guideline under standardised assumptions, rather than absolute predictions for any single location.

While empirical calibration with a specific existing building was not performed, such calibration would inherently bias the results toward the operational idiosyncrasies and construction defects of that single case, thereby limiting cross-climatic transferability. Instead, this study relies on the well-established 'comparative accuracy' of the EnergyPlus engine (Som and Gregory, 2011). In early-stage parametric design, the primary objective is not to predict

TABLE 1 Simulation parameters applied in DesignBuilder.

Category	Parameters	Specifications
Occupancy	Density	0.1497 people/m^2
	Activity	Lighter manual work (met factor = 0.90)
	Clothing insulation	summer: 0.50 clo; winter: 1.00 clo
Thermal control	Heating setpoint	20 °C (setback 12 °C)
	Cooling setpoint	24 °C (setback 28 °C)
Lighting	Power density	5.0 W/m^2 per 100 lux
	Control strategy	Linear dimming, range 0.1–1.0
	Glare limit	Daylight glare index (DGI) ≤ 22
Equipment	Office plug load	3.5 W/m^2 (scheduled use)
Envelope	Glazing	Double glazing: CLEAR 3 mm + AIR 13 mm + CLEAR 3 mm
	Walls	Brick (0.10 m) + XPS insulation (0.0795 m) + concrete block (0.10 m) + gypsum plaster (0.013 m)
	U-value	0.35 W/m^2·K

TABLE 2 Independent and dependent variables in the dataset.

Variable type	Name	Categories/Values	Purpose
Independent variables (inputs)	Plan ratio	1:1, 1:1.5, 1:2	Testing the influence of geometry on surface-to-volume ratios, daylight, and energy
	Façade configuration	Single-sided glazing; double-sided glazing	Assessing the impact of glazing layout and daylight/ventilation potential
	Window-to-wall ratio (WWR)	10%–100% (10% increments)	Identification of glazing thresholds for comfort and energy balance
	Orientation	0°–360° (15° intervals)	Capturing solar exposure and orientation-dependent loads
	Climate location	Nine representative cities (Köppen–Geiger zones)	Ensuring climatic diversity (tropical, arid, temperate, continental)
Dependent variables (outputs)	Discomfort hours (hr)	Annual hours outside the adaptive thermal comfort band	Measuring user comfort and learning suitability
	Total site energy consumption (kWh)	Heating, cooling, lighting, and equipment	Representing operational efficiency
	CO_2 emissions (kg)	Derived from site energy consumption	Capturing the environmental footprint of scenarios

the exact energy bill (absolute value) but to correctly rank the performance of design variants (relative difference). By adhering to international standard operational protocols (ASHRAE/ISO) rather than site-specific data, the framework ensures that observed performance shifts are attributable solely to passive design parameters (WWR, geometry, orientation) rather than to uncontrolled operational noise.

2.5 Analytical workflow

The analytical framework of this study was structured as a multi-stage workflow designed to transform a large, complex simulation dataset into actionable, climate-sensitive design knowledge. The dataset, comprising approximately 13,000 scenarios, combined discrete and continuous variables across geometry, envelope, orientation, and climate, which required a rigorous sequence of analytical steps to ensure internal validity, interpretability, and practical relevance. The workflow progressed from descriptive exploration to predictive modelling, optimisation, and robustness testing. Each stage was selected to address a specific gap: Exploratory Data Analysis (EDA) clarified baseline patterns and variability; machine learning quantified parameter influence and revealed non-linear interactions; multi-objective optimisation reconciled conflicting design goals; and robustness analysis tested whether the derived guidelines could withstand climatic diversity. All analyses were conducted in MATLAB R2024a to ensure consistency and reproducibility across the workflow.

2.5.1 Exploratory data analysis (EDA)

The first stage established a systematic understanding of the performance space defined by the dataset. The Exploratory Data

Analysis (EDA) stage was conducted using box plots and median-trend summaries to visualise data distributions, outliers, and cross-climatic variability (Tukey, 1977) (Lortie, 2017) (Chen, 2021). EDA was employed to examine the distribution and variability of discomfort hours, site energy consumption, and CO_2 emissions across the nine climatic contexts. This step was not merely descriptive but also diagnostic, allowing the detection of irregularities in the dataset, the assessment of the magnitude of cross-climatic variation, and the identification of preliminary associations between input variables and outcomes. For example, climates with high solar radiation intensity showed early signs of sensitivity to WWR increases, whereas temperate oceanic climates exhibited more stable performance across orientations. EDA thus provided the foundation for identifying where design decisions were likely to exert disproportionate influence, guiding the need for deeper modelling through machine learning. This stage was applied to diagnose the dataset and visualise the magnitude of cross-climatic differences. All procedures were carried out in MATLAB R2024a.

- Data preparation: Simulation outputs were imported with readtable; decimal separator inconsistencies were fixed, and faulty/missing records were removed. Analysis variables were defined as CO_2 emissions (kg), total site energy (kWh), and annual hours of discomfort (h). Climate was treated as a categorical city variable representing a Köppen–Geiger class.
- Box plots (boxplot/boxchart): Box plots were produced using Tukey whiskers (lower ≈ Q1–1.5·IQR, upper ≈ Q3+1.5·IQR) for each climate. Tukey fences are thresholds used to flag outliers (Tukey, 1977). Observations beyond the whiskers were flagged as potential outliers, enabling visual and systematic detection of anomalies in the dataset.
- Central tendency and spread summaries: Climate-wise medians were computed with groupsummary and reported in Table 3. Each box's IQR width (Q3–Q1) was interpreted as within-climate variability. Median shifts (deviations of climate medians from the overall median/differences across cities) provided a qualitative measure of between-climate magnitude. Wide IQRs indicated high dispersion; narrow IQRs indicated more stable performance.
- Diagnostic role and bridge to subsequent stages: The EDA was not only descriptive but diagnostic:
  i. identification of irregular/outlier observations;
  ii. making cross-climatic differences visible via medians and IQR;
  iii. observing preliminary relationships between design inputs and outcomes (e.g., sensitivity to increasing WWR in high-insolation climates). These findings informed the subsequent XGBoost + SHAP interpretation and multi-objective optimisation steps.

2.5.2 Machine learning (XGBoost + SHAP)

While EDA identifies patterns descriptively, it does not quantify the relative influence of variables or capture complex nonlinear interactions. To address this, the second stage applied Extreme Gradient Boosting (XGBoost), an ensemble learning technique well-suited to heterogeneous datasets with mixed categorical and continuous inputs (Chen and Guestrin, 2016) (Friedman, 2001).

In this study, Extreme Gradient Boosting (XGBoost) was employed to perform regression on tabular data comprising both continuous and categorical predictors. Gradient-boosted decision trees are well-suited to heterogeneous datasets because they capture strong nonlinear effects and interactions without requiring feature scaling. XGBoost controls overfitting through shrinkage, L1/L2 regularisation, and row/column subsampling. Thanks to its optimised tree growth and parallelisation, it trains efficiently and scalably across large design spaces (≈13k scenarios) (Chen and Guestrin, 2016; Friedman, 2001). Recent benchmarks show that, on tabular problems, tree-based ensembles often match or exceed SVMs and neural networks in accuracy and training stability while requiring far fewer hyperparameter tweaks (Chen and Guestrin, 2016; Shwartz-Ziv and Armon, 2022). In addition, tree ensembles provide exact, model-consistent explanations via TreeSHAP, whereas SVM/ANN models typically require more costly, model-agnostic approximations (Lundberg et al., 2020). For these reasons, XGBoost was adopted as the primary predictive model due to its suitability for the data characteristics, built-in regularisation, computational efficiency, and full explainability. The key XGBoost hyperparameters used in this study are summarised in Table 3.

All models were trained using gradient-boosted regression trees with a learning rate of 0.05 and 300 boosting iterations. Tree complexity was controlled through a minimum leaf size of 5, and all predictors were considered at each split. Categorical variables (climate zone, façade configuration, and plan ratio) were explicitly handled as categorical predictors. The dataset was randomly split into training (80%) and test (20%) subsets using a fixed random seed (rng = 42) to ensure reproducibility. Regularisation was implicitly achieved through shrinkage (learning rate) and tree structure constraints rather than explicit L1/L2 penalties. These settings were selected based on preliminary tuning experiments to balance predictive accuracy and generalisation.

Separate regression models were developed for each output: discomfort hours, total site energy use, and CO_2 emissions to ensure targeted predictive accuracy. Model performance was rigorously validated using R^2, which quantified explanatory power, and RMSE, which measured prediction error in absolute terms (Chai and Draxler, 2014). The trained models were further interrogated using Shapley Additive Explanations (SHAP) to address the "black box" problem typically associated with ensemble methods. SHAP provided a consistent framework for quantifying each variable's marginal contribution to model predictions (Lundberg and Lee, 2017; Lundberg et al., 2020). Partial Dependence Plots (PDPs) were subsequently employed to visualise non-linear relationships and identify critical thresholds in the model responses, focusing on the most influential variables identified by the SHAP analysis.

This dual application, XGBoost for predictive modelling and SHAP for interpretability, produced several critical insights. First, it established a clear hierarchy of variable importance, demonstrating that climate zone and WWR consistently emerged as the most influential performance drivers. In contrast, factors such as orientation exerted comparatively modest effects. Second, it revealed threshold behaviours, notably, increasing WWR beyond

TABLE 3 XGBoost hyperparameters.

Parameter	Value
Learning rate	0.05
Number of trees	300
Min leaf size	5
Max features per split	All
Train–test split	80%/20%
Random seed	42
Categorical handling	Native

approximately 40% in hot-arid climates led to a disproportionately sharp rise in cooling energy demand. Third, it uncovered interaction effects, showing, for example, that the performance penalties of high glazing ratios were amplified in continental climates but partially mitigated under humid subtropical conditions. These findings transformed raw simulation outputs into an interpretable framework of design sensitivities, thereby enabling the evidence-based identification of leverage points most critical for architectural decision-making.

2.5.3 Multi-objective optimisation

The third stage extended the analysis from explanatory insights to decision-oriented outcomes. Architectural design rarely optimises for a single objective; instead, practitioners must reconcile competing demands, such as comfort, energy efficiency, and environmental performance. A Pareto-based optimisation framework was employed to capture this complexity. Pareto-based multi-objective optimisation does not seek a single "best" point; instead, it yields the set of non-dominated solutions (the Pareto front) that cannot be improved in one objective without worsening at least one other. This front can be efficiently approximated with evolutionary algorithms, allowing decision-makers to select along the trade-off surface (Deb, 2001; Deb et al., 2002; Zitzler et al., 2001; Coello Coello, 2006). Rather than prescribing a single "best" solution, Pareto fronts were constructed to map the non-dominated solutions, where improvement in one metric inevitably incurred trade-offs in others. From these fronts, three archetypal strategies were extracted:

1. Comfort-prioritised solutions minimised discomfort hours even at higher energy or emissions cost.
2. Energy/CO_2-prioritised solutions, which reduced operational and environmental burdens, often at the expense of comfort.
3. Balanced solutions sought compromise across all objectives and are most aligned with holistic sustainability goals.

This stage provided a structured framework for navigating trade-offs, offering decision-makers flexibility in aligning strategies with local policy priorities, resource constraints, or user expectations. It should be noted that the Pareto fronts in this study were not generated using evolutionary multi-objective optimisation algorithms such as NSGA-II or SPEA2. Instead, a surrogate-based exhaustive evaluation approach was adopted. All feasible design combinations within the predefined parametric space were explicitly generated, and their performance values (CO_2 emissions, discomfort hours, and total site energy) were predicted using the trained machine learning models. Pareto-optimal solutions were then identified through direct dominance checking across the full candidate set. This deterministic Pareto filtering approach eliminates the need for population size, crossover operators, mutation rates, or generation numbers. It ensures that the resulting Pareto front represents the proper non-dominated set within the explored design space, rather than an approximation obtained through stochastic search.

2.5.4 Robustness analysis

The final stage tested whether the optimisation outcomes were stable across climates and thus transferable beyond single-context solutions. Robustness aims to reduce performance dispersion under uncertainty and/or to limit worst-case loss (Ben-Tal et al., 2009; Bertsimas et al., 2011; Beyer and Sendhoff, 2007). In this study, the mean–variance criterion is an engineering adaptation of Markowitz's $\mu+\lambda\sigma$ formulation, which rewards not only a low average score but also a slight standard deviation (Markowitz, 1952). In regret-based robustness, the goal is to minimise either the maximum (minimax regret) or the average of a candidate's relative loss with respect to the best solution in each climate (Savage, 1954; Kouvelis and Yu, 1997; Aissi et al., 2009). In multi-objective settings, the notion of a "robust Pareto" front has been examined in detail in the evolutionary multi-objective optimisation literature (Deb and Gupta, 2005). Robustness analysis assessed the variance in performance outcomes when strategies derived in one climatic zone were applied to others. This step identified which solutions were highly context-dependent and which demonstrated cross-climatic stability. In addition, a subset of global-optimum scenarios was defined, and strategies were designed that, while not always locally dominant, consistently ranked in the top tier across multiple climates. This analysis was crucial for advancing the study from context-specific recommendations to generalised design guidelines. The research provided a framework for practitioners to adapt flexibly according to project location and design priorities, distinguishing between climate-sensitive (i.e., tailored to a particular region) and climate-resilient (i.e., robust across regions) strategies.

For each candidate design obtained from the optimisation, a composite performance score was calculated in each of the nine climates. CO_2, energy and discomfort indicators were first brought to the same scale within each environment (0–1, min–max normalisation) and combined with equal weights into a single score. Then two complementary checks were applied:

1. Mean–variance approach: For each candidate, the cross-climate average and variability (standard deviation) of the score were computed. The design that achieved a low average score with slight variation across climates was selected as "robust." To reflect "balance," the penalty on variability was set to $\lambda = 0.5$. The candidate's detailed CO_2, energy, and discomfort values in each climate are reported in Tables 7–8.

2. Regret approach: Relative to the best local solution in each climate, the extent to which each candidate lagged was computed. Two measures were used:
   - Minimax regret: minimises a candidate's loss in the worst climate (risk-averse).
   - Average regret: minimises the average loss across all climates (risk-neutral).

The robust solutions identified by these two criteria are summarised in the table.

All procedures were automated in MATLAB; climate-wise scores were generated, and mean/standard deviation values, as well as regret values, were calculated for each candidate. The designs with the lowest values were flagged and exported to the tables.

2.6 Evaluation metrics

The evaluation of passive design strategies requires a set of metrics that capture performance in a manner that is both technically rigorous and meaningful for practical application. This study defined four complementary metric categories: energy efficiency, environmental sustainability, thermal comfort, and the interpretability of optimisation outputs. Together, these measures provided a multidimensional basis for assessing the effectiveness of design decisions in library reading halls, where user wellbeing, operational efficiency, and sustainability are inseparably linked.

2.6.1 Energy performance (kWh)

Annual site energy consumption, expressed in kilowatt-hours, was calculated by summing the demands for heating, cooling, lighting, and equipment loads. This indicator is widely used in building performance simulation and reflects the direct operational efficiency of the design. Its selection was motivated by the fact that libraries typically operate for extended hours and accommodate high occupant densities, leading to continuous demands on HVAC and lighting systems. Quantifying energy performance across various scenarios provided a robust basis for comparing how geometric and envelope parameters influence operational loads under diverse climatic conditions.

2.6.2 Environmental impact (kg CO_2)

To extend the analysis beyond energy use, total site energy was converted into equivalent carbon dioxide emissions using established emission factors. Expressing results in kilograms of CO_2 enabled the direct assessment of the environmental footprint of design choices. This metric addresses the pressing need for climate change mitigation strategies in the built environment, as underscored by international targets such as the Paris Agreement. Including CO_2 alongside kWh values ensured that strategies were not only efficient in reducing energy demand but also aligned with global decarbonisation priorities.

In all simulations, the HVAC system supplied heating energy via natural gas, while the cooling and auxiliary systems (including lighting and equipment) were powered by electricity. Total site energy consumption was defined as the sum of final energy use associated with these different energy carriers.

CO_2 emissions were calculated within the DesignBuilder interface using the EnergyPlus simulation engine and were based on fuel-specific emission factors assigned to heating and electricity consumption. The use of city-specific EPW climate files altered the relative distribution of heating and cooling loads across climates, thereby modifying the proportion of natural gas and electricity consumption. As a result, CO_2 emissions vary across climates even when total site energy consumption is comparable.

In this context, CO_2 emissions were treated as an environmental performance indicator representing the climate impact of energy demand. Emission factors for natural gas were applied to heating-related energy use, while electricity emission factors were applied to cooling, lighting, and equipment loads. This approach ensures that CO_2 emissions reflect not only the magnitude of energy consumption but also its energy composition (fuel mix).

Although electricity grid carbon intensity varies by country and region, incorporating location-specific grid factors would introduce additional energy-supply-related variability and weaken the study's climate- and envelope-focused comparative structure. Therefore, energy supply parameters were held constant, and the analysis was deliberately structured to isolate the effects of climatic conditions and passive design parameters on building performance.

2.6.3 Thermal comfort (discomfort hours)

Thermal comfort was assessed regarding the annual number of hours when indoor operative temperatures fell outside the adaptive thermal comfort band. This user-centred indicator was chosen over more abstract indices (e.g., PMV) because it directly quantifies the duration of exposure to unacceptable thermal conditions. In the context of library reading halls, where users often remain seated for prolonged periods, comfort has a significant impact on both health and cognitive performance. The study ensured that energy reductions were not pursued at the expense of learning suitability and user wellbeing by adopting discomfort hours as a key measure.

Thermal comfort was calculated as the annual occupied hours outside the adaptive comfort band. The band's centre is determined by the adaptive model, which responds to outdoor conditions, so that thresholds self-adjust according to climate rather than applying a uniform fixed range across tropical, arid, and continental contexts. The centre of the band is set by the adaptive model, which responds to outdoor conditions. This means that the thresholds automatically adjust to local climate conditions rather than applying a fixed range across tropical, arid, and continental contexts.

In line with international practice, the 80% acceptability band was adopted, consistent with EN 16798-1 (BSI, 2009) and ASHRAE 55 (ASHRAE, 2020a). A metabolic rate of ≈0.9 met was assumed for sedentary library users, with seasonal clothing levels of 0.50 clo (summer) and 1.00 clo (winter), consistent with the DesignBuilder/EnergyPlus 'All Clothing' setting.

This user-centred indicator directly measures the duration of exposure to unacceptable conditions, in contrast to more abstract indices such as PMV, and aligns with hour-based overheating/underheating metrics widely used in CIBSE TM52/TM59 (CIBSE, 2013; CIBSE, 2017), EN 16798-1 (BSI, 2009), and ASHRAE 55 (ASHRAE, 2020a). In this way, energy and CO_2 reductions are

pursued without compromising learning suitability and user wellbeing.

2.6.4 Optimisation outputs

Finally, the analysis incorporated a set of decision-oriented metrics derived from the machine learning and optimisation stages. These included Pareto-optimal solutions, which captured the trade-offs between comfort, energy, and emissions without privileging a single outcome; SHAP values, which quantified the relative influence of each design parameter and provided interpretable rankings to guide priorities; and critical thresholds identified through partial dependence analysis, such as glazing ratios beyond which energy penalties rose disproportionately. The inclusion of these outputs enhanced the study's explanatory and prescriptive power. While energy, CO_2, and comfort metrics quantify performance outcomes, optimisation-derived indicators reveal the mechanisms and leverage points behind those outcomes, thereby making the results directly actionable for design decision-making.

The evaluation framework addressed performance across the scales of efficiency, sustainability, usability, and decision relevance by integrating energy (kWh), environmental (kg CO_2), comfort (hours of discomfort), and optimisation-derived outputs. This multidimensional approach ensured that the study's findings not only advanced theoretical understanding but also delivered evidence-based, practice-oriented guidelines for climate-adaptive library design.

3 Results

3.1 Exploratory data analysis (EDA)

An exploratory data analysis (EDA) was first carried out to provide a descriptive baseline of performance outcomes across climates, forming the foundation for subsequent machine learning and optimisation. This step was necessary for two reasons: to simplify the extensive dataset of various scenarios by visualising key trends; and to highlight the magnitude and direction of climate-driven differences as the dominant explanatory factor. By integrating boxplots and median summaries, the analysis enabled the characterisation of intra-climatic variability while providing representative central tendencies to support robust cross-climatic comparisons.

Figure 4 presents the distributions of annual CO_2 emissions, discomfort hours, and total site energy consumption across the nine cities, while Table 4 summarises the corresponding medians. Results show that tropical humid climates exhibit the highest median values for both energy use and emissions, with Singapore (8679 kg CO_2; 14,321 kWh) and Goa (8448 kg CO_2; 13,941 kWh) also recording elevated discomfort hours (2563 h and 1889 h, respectively). At the other extreme, hot-arid Al-Madinah shows much lower energy demand (9160 kWh) and emissions (5551 kg), with only 429 discomfort hours, reflecting the predominance of cooling loads. Cold desert (Turpan) and humid continental (Ann Arbor) climates exhibit relatively high discomfort levels (2285 h and 2600 h), highlighting the challenges of long heating seasons despite moderate-to-high energy demands. Phoenix (hot semi-arid) and İzmir (Mediterranean) occupy intermediate positions, while London (oceanic) and Shanghai (humid subtropical) reveal high median discomfort values (>2500 h) despite moderate energy and CO_2 levels, underscoring that climatic moderation does not automatically ensure comfort.

The distributional patterns in Figure 4 further reinforce these findings. Tropical (Singapore, Goa) and extreme desert (Turpan) climates exhibit the widest interquartile ranges, indicating that performance outcomes in these regions are highly susceptible to passive design parameters, such as the window-to-wall ratio (WWR) and orientation. In contrast, Phoenix and İzmir display narrower spreads, suggesting more stable performance across design variations. In colder climates, such as Ann Arbor, wide variability in discomfort hours reflects the difficulty of consistently meeting heating requirements.

In summary, Figure 4 presents box plots with conventional whisker limits (Q1–1.5·IQR; Q3+1.5·IQR), highlighting distributional irregularities across climates. The medians reported in Table 4 and IQR widths further quantify these differences: tropical and extreme desert climates show broad IQRs, indicating high variability, whereas Mediterranean and semi-arid contexts exhibit narrower ranges, reflecting more stable performance. The EDA confirms that climate is the dominant determinant of comfort, energy demand, and emissions. However, the breadth of distributions in specific contexts highlights where design parameters can exert disproportionate influence.

3.1.1 Statistical significance of climate-driven differences

To complement the descriptive exploratory data analysis, non-parametric statistical tests were conducted to examine whether the observed differences across climate zones were statistically significant. Given that the performance indicators did not satisfy normality assumptions and involved multiple independent climate groups, the Kruskal–Wallis H test was applied.

The results indicate statistically significant differences across climate zones for all three performance indicators: annual CO_2 emissions ($\chi^2 = 9666.05$, df = 8, $p < 0.001$), annual discomfort hours ($\chi^2 = 9800.12$, $p < 0.001$), and total site energy consumption ($\chi^2 = 9800.12$, $p < 0.001$) (Table 5). These findings confirm that climate exerts a dominant, statistically robust influence on building energy use, emissions, and thermal comfort.

Post-hoc pairwise comparisons using the Dunn–Šidák correction further revealed that most climate-zone pairs differ significantly, particularly between tropical, arid, and continental climates. This statistical evidence substantiates the distributional patterns observed in the boxplots and medians, reinforcing the conclusion that climate is the primary determinant shaping performance variability, while design parameters act as secondary modifiers within each climatic context. Accordingly, the exploratory analysis provides not only descriptive but also inferential support for the climate-driven structure of the dataset, justifying the subsequent application of machine learning and multi-objective optimisation to disentangle design sensitivities within and across climate classes.

In all Kruskal–Wallis tests, the degrees of freedom were equal to eight, corresponding to the 9 Köppen–Geiger climate classes analysed (df = k − 1). These descriptive insights provide a

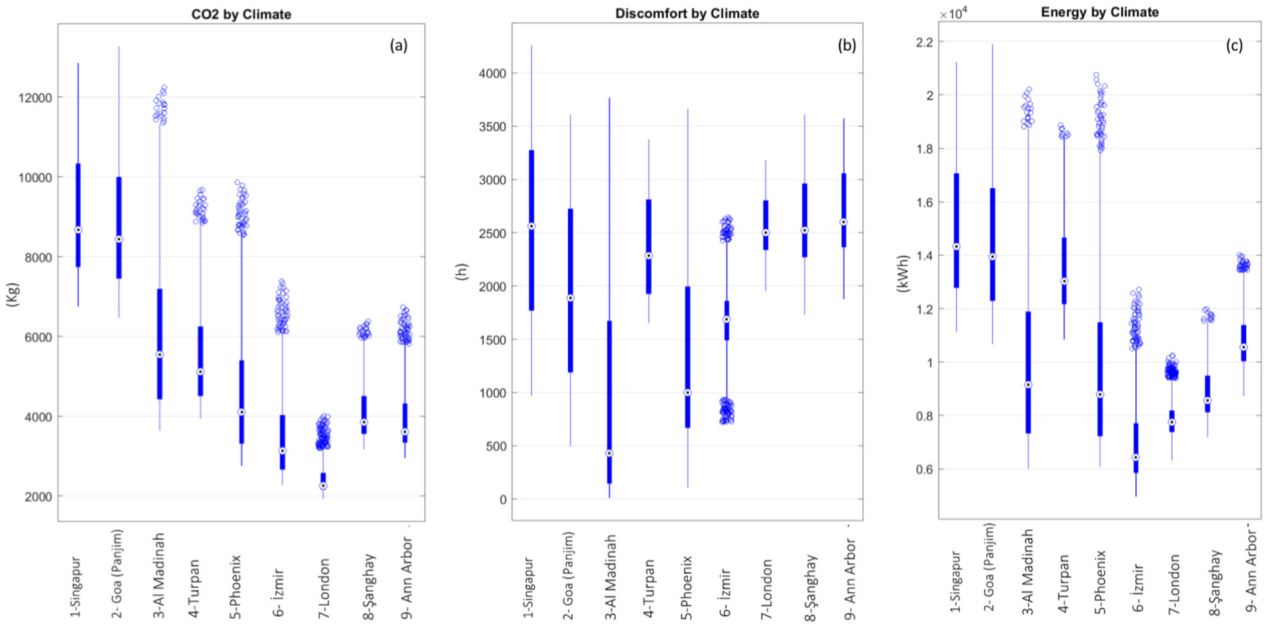


FIGURE 4
Distributions across climate zones: **(a)** annual CO_2 emissions, **(b)** annual discomfort hours, and **(c)** annual total site energy consumption.

TABLE 4 **Median annual CO_2 emissions (kg), discomfort hours (h), and total site energy (kWh) across climate zones.**

Climate zone	CO2 (kg)	Discomfort hour (h)	Total site energy (kWh)
1- Singapore	8678.54	2563.25	14321.04
2- Goa (Panjim)	8448.02	1889.25	13940.65
3- Al-Madinah	5550.90	428.75	9160.08
4- Turpan	5113.22	2284.50	13030.14
5 - Phoenix	4103.48	999.00	8790.67
6- İzmir	3132.78	1685.50	6419.43
7- London	2254.64	2502.50	7743.24
8- Shanghai	3856.15	2521.75	8564.52
9- Ann Arbor	3610.79	2600.25	10561.38

transparent foundation for the subsequent machine learning and optimisation analyses, which formally disentangle parameter importance and identify robust climate-adaptive solutions.

3.2 Machine learning model performance

The exploratory data analysis revealed climate as the dominant factor shaping performance outcomes. Extreme Gradient Boosting (XGBoost) models were applied to CO_2 emissions, discomfort hours, and site energy consumption to quantify the relative influence of design parameters and capture non-linear interactions.

Table 6 reports the predictive accuracy of the models. All three achieved excellent performance, with R^2 values exceeding 0.95 for both training and test datasets. The CO_2 model showed the strongest predictive power (R^2_train = 0.996, R^2_test = 0.996; RMSE_train = 152.47, RMSE_test = 158.14), followed by the energy model (R^2_train = 0.992, R^2_test = 0.992; RMSE_train = 304.46, RMSE_test = 320.72). The discomfort model was slightly less accurate but still robust (R^2_train = 0.960, R^2_test = 0.956; RMSE_train = 182.97, RMSE_test = 190.95). These values confirm that the models successfully captured non-linear relationships and produced predictions with small residual errors relative to the scale of the outcomes, making them reliable for decision-support applications.

3.2.1 Parameter importance (SHAP analysis)

Although ensemble models deliver high predictive accuracy, their interpretability remains limited. Shapley Additive Explanations (SHAP) were employed to attribute predictions to individual parameters, thereby overcoming this limitation. Figure 5 presents SHAP summary plots for CO_2 emissions, discomfort hours, and total site energy consumption.

Across all outputs, climate zone emerged as the overwhelmingly dominant predictor, surpassing all other design parameters. This confirms the previous findings and reinforces the central role of climate in determining building performance. Among design parameters, the window-to-wall ratio (WWR) consistently ranked second in importance, followed by façade configuration. WWR exerted a bidirectional influence: higher values tended to increase cooling and heating loads (raising emissions and energy demand), but very low WWR values also led to higher discomfort due to poor daylight access and ventilation. Façade configuration moderated these effects by altering solar gain and transmission dynamics.

By contrast, orientation and plan ratio contributed less overall but still showed notable effects in specific contexts. Orientation mattered most in climates with strong solar asymmetry, such as Al-Madinah, where east–west exposures generated higher cooling loads. Plan ratio showed subtler but systematic impacts, particularly by altering surface-to-volume ratios and daylight penetration in compact versus elongated forms. Taken together, the SHAP analysis reveals a robust hierarchy of influences, with climate exerting the strongest effect, followed by WWR, façade configuration, and, to a lesser extent, orientation and plan ratio.

3.2.2 Critical thresholds

Partial Dependence Plots (PDPs) were generated to complement the SHAP analysis, examine non-linear relationships, and identify threshold behaviours. Figure 6 shows PDP curves for WWR and orientation, while categorical comparisons are reported for plan ratio and façade configuration.

- WWR thresholds:
  - For CO_2 emissions (Figure 6a) and energy consumption (Figure 6c), values increased nearly monotonically with WWR; however, inflection points were identified at approximately 56.4% and 83.6%, where the slope steepened markedly, indicating disproportionate penalties at high glazing ratios.
  - A U-shaped curve was observed for discomfort hours (Figure 6b). Very low WWR values (<13.6%) were associated with elevated discomfort, which decreased as the WWR moved into the mid-range before rising beyond approximately 60%.
  - Together, these patterns suggest that the mid-range of WWR (30%–40%) represents a balanced zone across climates, minimising discomfort while avoiding steep increases in energy and emissions.

The proposed 30%–40% WWR band is consistent with the cross-climate average of knee-based breakpoints observed on the global PDP curves and, rather than seeking a single "point optimum," adopts a climate-adaptable design-corridor approach. This corridor (i) coincides with the mid-range where the discomfort curve approaches its minimum, (ii) maintains a safe distance from the sharp increases in CO_2 and energy observed at ≈56% and above, and (iii) will be compared against the knee/minimax-regret findings reported in the subsequent sections from multi-objective optimisation and robustness analyses. The contemporary literature likewise shows that the daylight–energy balance is most rational at mid WWR values, whereas high WWR rapidly increases cooling loads and glare risk (Yu et al., 2008; (Ochoa et al., 2012b; Tzempelikos and Athienitis, 2007). Accordingly, the 30%–40% range is proposed not as a universal "optimum," but as a practical and safe starting point across various climates; final values should be refined to the project context using multi-objective and robustness analyses.

TABLE 5 Kruskal–Wallis test results for performance indicators across climate zones.

Target variable	χ^2 statistic	df	p-value
CO_2 emissions	9666.05	8	<0.001
Discomfort hours	9800.12	8	<0.001
Total site energy	9800.12	8	<0.001

TABLE 6 Accuracy comparison of the models (R^2_train, R^2_test, RMSE_train, RMSE_test).

Target	R2_train	R2_test	RMSE_train	RMSE_test
CO_2	0.996	0.996	152.47	158.14
Discomfort	0.960	0.956	182.97	190.95
Energy	0.992	0.992	304.46	320.72

- Orientation thresholds:
  - Energy and CO_2 both reached minima near approximately 342°, with knee points at approximately 42° and 153°.
  - Discomfort showed a local minimum at approximately 192°, with a knee point at approximately 258°.
  - These findings confirm that orientations near north–south generally perform more stably, while east–west exposures remain consistently disadvantageous.
- Plan ratio:
  - Systematic differences were observed across categories. Type-1 plans produced the lowest CO_2 emissions and energy consumption, while Type-2 plans yielded the lowest discomfort hours. Type-3 plans performed worst across all metrics. The differences between the best- and worst-performing classes were 116.46 kg for CO_2, 228.33 kWh for energy, and 15.02 h for discomfort.
- Façade configuration:
  - A strong separation was evident between façade types. The Single configuration consistently outperformed the Double Configuration, with maximum differences of 1527.22 kg CO_2, 255.80 h of discomfort, and 2516.11 kWh of energy.

3.2.3 Methodological considerations

PDPs provide marginal average effects for each parameter, meaning that interaction effects (e.g., WWR × Climate or WWR × Façade) may be smoothed out. As such, the threshold values identified here should be interpreted as guiding values rather than

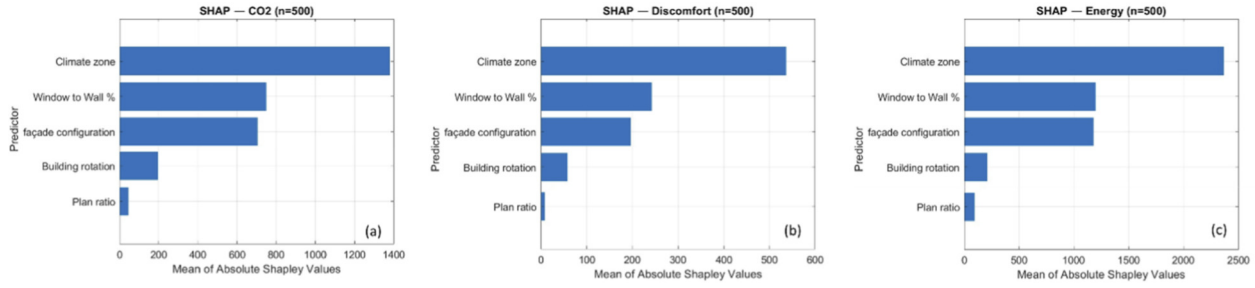


FIGURE 5
SHAP summary plots: **(a)** CO_2 emissions (kg), **(b)** discomfort hours (h), and **(c)** total site energy (kWh).

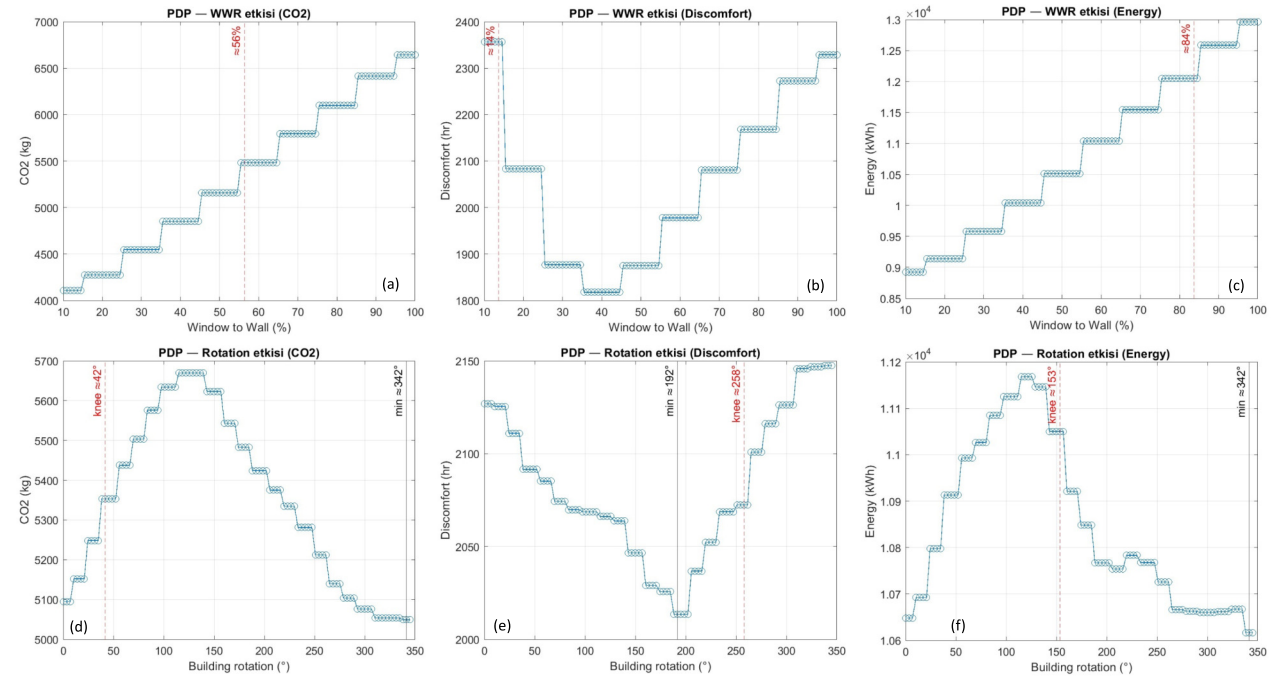


FIGURE 6
Partial dependence (PDP) curves and critical thresholds for the XGBoost models: **(a)** WWR–CO_2, **(b)** WWR–discomfort hours, **(c)** WWR–total site energy, **(d)** orientation–CO_2, **(e)** orientation–discomfort hours, and **(f)** orientation–total site energy. The red dashed line marks the critical threshold (knee point) where the absolute second derivative reaches its maximum.

universal optima. Their robustness is further evaluated in the multi-objective optimisation and cross-climatic robustness analysis.

The machine learning analysis extends the descriptive findings of Section 3.1 by quantifying the influence of parameters and identifying thresholds. Climate is confirmed as the dominant driver, but WWR, façade type, orientation, and plan ratio all exert systematic, measurable effects. Key thresholds were identified for WWR (13.6%, 56.4%, 83.6%), orientation (42°, 153°, 192°, 258°, 342°), plan ratio (Type-1 for energy/CO_2, Type-2 for comfort, Type-3 worst), and façade configuration (Single outperforming Double). These results establish a clear hierarchy of influences and provide the quantitative foundation for multi-objective optimisation, where performance trade-offs are explicitly addressed.

3.3 Multi-objective optimisation

The problem was formulated as a multi-objective optimisation problem because CO_2 emissions, discomfort hours, and total site energy consumption cannot be minimised simultaneously. In this framework, XGBoost-based surrogate models were combined with Pareto dominance principles to identify non-dominated design alternatives, eliminating solutions in which improvement in one objective necessarily resulted in deterioration in at least one other objective.

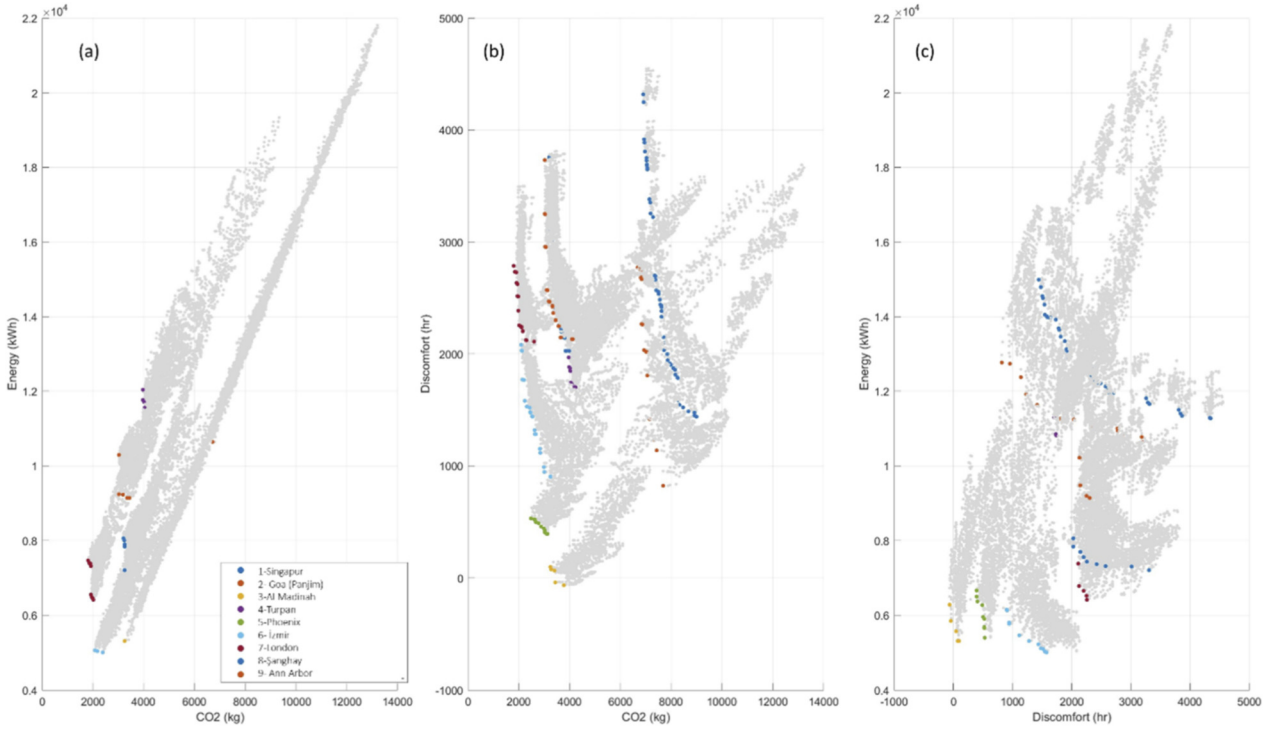


FIGURE 7
Pareto fronts in the two-objective planes: **(a)** CO_2–energy, **(b)** CO_2-discomfort and **(c)** discomfort–energy.

The Pareto-optimal candidates were visualised using both two-objective projections and the full three-dimensional objective space. It should be emphasised that the Pareto fronts presented in this study do not represent approximated solutions obtained through evolutionary or stochastic sampling methods. Instead, they correspond to the exact set of non-dominated solutions derived from an exhaustive evaluation of all feasible design combinations within the predefined design space.

3.3.1 Two-objective trade-offs

Figure 7 presents the two-objective Pareto fronts: (a) CO_2–energy, (b) CO_2-discomfort, and (c) discomfort–energy. Grey points represent all simulated candidates, while coloured points denote Pareto-optimal solutions by climate.

- CO_2–energy (Figure 7a): A strong near-linear relationship is observed, reflecting the derivation of CO_2 from energy use. The Pareto boundary runs along the lower-left edge of the distribution. Knee points are visible where further reductions in CO_2 require disproportionately large increases in energy. The slope and position of the front vary across climates, confirming that differences in heating/cooling loads, as well as emission factors, shift the trade-off space. The relationship between total energy consumption and CO_2 emissions arises from the fact that energy demand is met through different fuel mixes depending on climatic conditions, natural gas for heating and electricity for cooling and auxiliary systems. Therefore, a strong near-linear relationship between energy consumption and CO_2 emissions is expected. However, this does not imply that the two objectives are identical. In addition to the magnitude of energy consumption, CO_2 emissions also reflect the type of energy carriers supplying this demand. In the DesignBuilder–EnergyPlus simulations, city-specific EPW climate files determine the distribution of heating and cooling loads, while CO_2 emissions are calculated using fuel-specific emission factors. As a result, design solutions with similar total energy consumption levels may still exhibit different CO_2 emission profiles due to climate-driven differences in fuel use.
- CO_2–discomfort (Figure 7b): A pronounced curvature is visible. In the low-CO_2, low-discomfort region, improvements are possible up to a knee point beyond which further CO_2 reductions sharply increase discomfort. The spread of grey points indicates substantial variability in candidate solutions, while climate-coloured Pareto fronts suggest that the trade-off rate varies across regions.
- Discomfort–energy (Figure 7c): A clear trade-off emerges, with reduced energy generally associated with higher discomfort. Knee points again delineate the transition where small comfort gains require considerable energy sacrifices. Climates dominated by cooling tend to show steeper slopes, while heating-dominant and temperate climates exhibit flatter profiles.

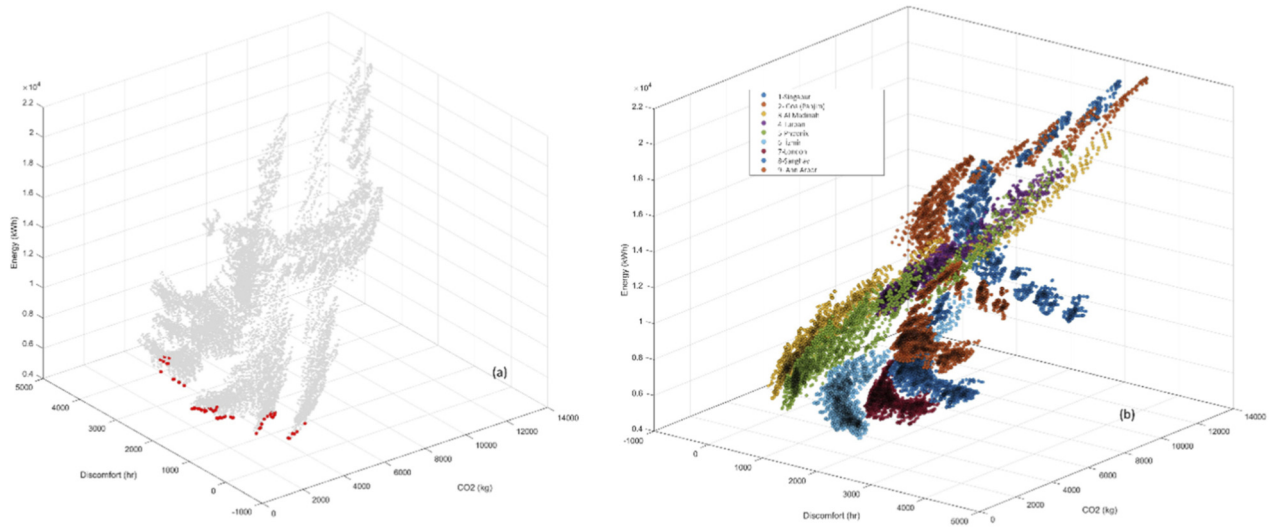


FIGURE 8
(a) Three-objective Pareto front (3D) for CO_2 emissions, discomfort hours, and total site energy. **(b)** Full objective space colour-coded by climate, illustrating clustering of candidates and differences in their positions across climates.

TABLE 7 **Global archetypal Pareto-optimal solutions: comfort-focused, energy/CO_2-focused, and balanced.**

Archetype (scenario)	Window to wall %	Building rotation (°)	Climate zone	Façade configuration	Plan ratio	CO_2 (kg)	Discomfort (hr)	Energy (kWh)
Comfort-focused	60	0	3-Al-Madinah	Single	Type-1	3431.1	38.89	5843.3
Energy/CO_2-focused	20	15	Phoenix	Single	Type-1	2467.7	531.31	5396.4
Balanced	10	15	3-Al-Madinah	Single	Type-1	3270.9	77.20	5313.6

These pairwise projections confirm that no single solution dominates across objectives and that trade-offs intensify beyond critical knee regions.

3.3.2 Three-objective pareto frontier

Figure 8a visualises the full three-dimensional Pareto front, where red points denote non-dominated candidates. The frontier forms a triangular surface that illustrates the simultaneous conflict among comfort, energy, and CO_2. The clustering of points is relatively limited but dense, implying that only a restricted subset of design combinations achieves balanced trade-offs. Local curvature on the surface corresponds to the knees observed in 2D projections, identifying critical thresholds where marginal costs increase sharply.

Figure 8b, colour-coded by climate, highlights that Pareto clustering is strongly climate-dependent. Tropical climates (Singapore, Goa) occupy high CO_2–energy regions, hot-arid climates (Al-Madinah, Phoenix) cluster at low CO_2–energy ends with variable comfort, temperate climates (London, Shanghai, İzmir) distribute more evenly near the centroid, and cold/continental climates (Ann Arbor, Turpan) lie toward higher discomfort values. Within each cluster, design parameters such as WWR, orientation, façade, and plan ratio provide fine-tuning, while climate establishes the overall position.

3.3.3 Global archetypal solutions

Three global archetypes were extracted from the Pareto frontier to represent distinct design priorities. Table 7 summarises their parameter sets and predicted performance:

- Comfort-focused archetype (Al-Madinah; WWR = 60%, orientation = 0°, Single façade, Type-1 plan): achieved a considerable reduction in discomfort (−38.9 h relative to baseline) but incurred higher CO_2 (3431 kg) and energy (5843 kWh).
- Energy/CO_2-focused archetype (Phoenix; WWR = 20%, orientation = 15°): produced the lowest energy (5,396 kWh) and emissions (2,468 kg), but with high discomfort (>530 h).
- Balanced archetype (Al-Madinah; WWR = 10%, orientation = 15°): achieved compromise values across metrics (3271 kg CO_2, 77 h discomfort, 5314 kWh energy).

These archetypes illustrate the fundamental conflicts among objectives and the need to prioritise trade-offs.

TABLE 8 Climate-specific archetypes selected from the Pareto front (parameters: WWR, orientation, façade, plan; performance: CO_2, discomfort, total site energy).

Window to wall %	Building rotation (°)	Climate zone	Climate code	Façade configuration	Plan ratio	CO_2 (kg)	Discomfort (hr)	Energy (kWh)	Reptype
10	150	Singapore	1	Single	Type-1	6889.2	4320.5	11349	CO2-min
100	90	Singapore	1	Single	Type-2	8990.3	1440.4	14985	DIS-min
10	165	Singapore	1	Single	Type-1	6889.4	4343.0	11269	ENG-min
40	150	Singapore	1	Single	Type-2	7415.1	2600.4	12023	Balanced (knee)
20	345	Goa (Panjim)	2	Single	Type-2	6670.8	2773.4	10932	CO2-min
100	0	Goa (Panjim)	2	Single	Type-1	7675.6	821.02	12763	DIS-min
10	15	Goa (Panjim)	2	Single	Type-1	6713.8	3186.5	10639	ENG-min
40	0	Goa (Panjim)	2	Single	Type-1	6928.5	2035.2	11238	Balanced (knee)
20	15	Al-Madinah	3	Single	Type-1	3250.5	98.671	5313.3	CO2-min
20	15	Al-Madinah	3	Single	Type-2	3773.0	63.404	6278.7	DIS-min
20	15	Al-Madinah	3	Single	Type-1	3250.5	98.671	5313.3	ENG-min
60	0	Al-Madinah	3	Single	Type-1	3431.1	38.893	5843.3	Balanced (knee)
10	15	Turpan	4	Single	Type-1	3965.5	1967.4	12031	CO2-min
20	165	Turpan	4	Single	Type-3	4236.4	1701.7	11298	DIS-min
20	165	Turpan	4	Single	Type-2	4083.0	1735.5	10815	ENG-min
20	195	Turpan	4	Single	Type-2	4052.0	1739.6	10815	Balanced (knee)
20	15	Phoenix	5	Single	Type-1	2467.7	531.31	5396.4	CO2-min
20	165	Phoenix	5	Single	Type-3	3125.7	392.50	6662.0	DIS-min
20	15	Phoenix	5	Single	Type-1	2467.7	531.31	5396.4	ENG-min
20	345	Phoenix	5	Single	Type-1	2666.2	499.71	5954.9	Balanced (knee)
20	15	İzmir	6	Single	Type-1	2082.8	2081.2	5063.0	CO2-min
80	180	İzmir	6	Single	Type-2	3250.8	902.84	6156.1	DIS-min
20	165	İzmir	6	Single	Type-1	2384.4	1572.7	5002.4	ENG-min
30	180	İzmir	6	Single	Type-2	2439.6	1478.3	5121.0	Balanced (knee)
60	15	London	7	Single	Type-1	1804.4	2788.1	7473.9	CO2-min
100	195	London	7	Single	Type-1	2599.8	2112.0	7387.7	DIS-min
60	180	London	7	Single	Type-2	2007.6	2255.3	6409.9	ENG-min
60	195	London	7	Single	Type-2	2005.7	2257.1	6409.9	Balanced (knee)
20	15	Shanghai	8	Single	Type-2	3196.2	3756.0	8061.1	CO2-min
100	180	Shanghai	8	Single	Type-2	3974.6	2026.5	8058.3	DIS-min
20	180	Shanghai	8	Single	Type-2	3269.6	3304.1	7210.8	ENG-min
40	195	Shanghai	8	Single	Type-2	3321.8	2568.6	7315.7	Balanced (knee)
20	15	Ann Arbor	9	Single	Type-1	3024.0	3730.1	10297	CO2-min

(*Continued*)

TABLE 8 Continued

Window to wall %	Building rotation (°)	Climate zone	Climate code	Façade configuration	Plan ratio	CO_2 (kg)	Discomfort (hr)	Energy (kWh)	Reptype
90	180	Ann Arbor	9	Single	Type-1	4128.5	2132.6	10214	DIS-min
70	180	Ann Arbor	9	Single	Type-2	3454.9	2300.5	9133.6	ENG-min
50	195	Ann Arbor	9	Single	Type-2	3182.4	2469.2	9227.7	Balanced (knee)

TABLE 9 Robust design identified under the mean–variance criterion (λ = 0.5; balanced weighting across objectives).

Window to wall %	Building rotation (°)	Façade configuration	Plan ratio	CO_2_mean (kg)	DIS_mean (hr)	ENG_mean (kWh)
60	195	Single	Type-2	4536.4	1614.9	9084.1

3.3.4 Climate-specific archetypes

Table 8 details climate-specific archetypes, each defined by WWR, orientation, façade, and plan ratio, with corresponding outputs. Several systematic patterns emerge:

- Tropical climates (Singapore, Goa): CO_2- and energy-minimising solutions clustered at very low WWR (≈10–20%), Single façades, and Type-1 plans. Comfort-minimising solutions required very high WWRs (>80–100%) and often Type 2/3 plans, at the cost of higher emissions. Balanced solutions stabilised around WWR = 40%, combining Single façades and orientations near 15°–20° or ~340°.
- Hot-arid climates (Al-Madinah, Phoenix): Optimal candidates converged at moderate WWR values (≈20–30%). Energy/CO_2-focused solutions selected compact Type-1 plans with Single façades, while comfort-focused cases allowed higher WWR (≈60%).
- Mediterranean climate (İzmir): Balanced archetypes clustered around WWR = 30–40% with Single façades and Type-1/2 plans. Energy minima occurred at WWR = 20%, while comfort-focused cases favoured WWR ≈80%.
- Temperate climates (London, Shanghai): Broader distributions were observed. London's CO_2 minima aligned with WWR ≈60% and specific orientations, while comfort minima approached fully glazed scenarios (≈100%). Shanghai had a balanced WWR between 20% and 40%, with comfort again associated with higher glazing ratios.
- Cold/continental climates (Turpan, Ann Arbor): All archetypes reported discomfort for more than 1700 h annually. Energy and CO_2 minima occurred at low WWR (20%), Single façades, and Type-1 plans, while balanced solutions required moderate WWR increases (40%–50%) to mitigate daylight deficits.

The optimisation results demonstrate that:

- Trade-offs among comfort, energy, and CO_2 are unavoidable.
- Knee points in Pareto fronts identify thresholds where marginal trade-offs become steep.
- Three global archetypes (comfort-, energy/CO_2-, and balanced-focused) illustrate distinct optimisation priorities.
- Climate-specific archetypes reveal divergent pathways: tropical climates oscillate between very low and very high WWR values; arid and Mediterranean climates converge on moderate WWR bands; temperate climates exhibit broad solution spaces; and cold/continental climates remain constrained by persistent discomfort.

These results confirm that optimisation outcomes are inherently climate-dependent and cannot be generalised globally. They establish the basis for further robustness analysis, where the stability of these archetypes is tested across multiple climates.

3.4 Robustness analysis

Optimisation identified climate-specific archetypes (Section 3.3), but architectural decision-making often requires effective strategies across multiple climates. To address this, robustness was evaluated using a mean–variance criterion (λ = 0.5, equal weighting of objectives after normalisation) and regret analysis (comparing candidates to local climate optima). These complementary methods identify designs that maintain acceptable performance across contexts rather than excelling only in a single climate.

3.4.1 Mean–variance criterion

The mean–variance analysis selected a robust candidate defined by WWR = 60%, orientation = 195°, Single façade, and Type-2 plan ratio. Table 9 reports its average performance across climates: CO_2 ≈ 4.54 t, discomfort ≈1615 h, and energy ≈9.08 MWh.

Table 10 illustrates the candidate's performance in each climate. It ranked highest in Mediterranean and arid contexts such as İzmir (score = 0.1254), Phoenix (0.1770), and Al-Madinah (0.185), where both CO_2 and energy were low, and discomfort remained moderate. In contrast, scores were weaker in humid tropical climates (Singapore = 0.485, Goa = 0.435) due to elevated energy use. In colder regions, such as Ann Arbor (0.303) and Turpan (0.358), discomfort exceeded 1900 h.

TABLE 10 Climate-specific performance of the mean–variance (λ = 0.5) robust design (lower values indicate better performance).

Order	Climate	Score	CO_2 (kg)	Discomfort (h)	Energy (kWh)
1	6-İzmir	0.1254	2865	1116.1	5467.8
2	5-Phoenix	0.17697	3822.3	709.23	8137.3
3	3-Al-Madinah	0.18478	5041.5	253.6	8398.9
4	7-London	0.20144	2005.7	2257.1	6409.9
5	8-Shanghai	0.26811	3588.2	2258.2	7437.6
6	9-Ann Arbor	0.30266	3349.9	2364.9	9141.6
7	4-Turpan	0.35813	4572.2	1997.1	11478
8	2-Goa (Panjim)	0.4351	7697.8	1487.9	12613
9	1-Singapore	0.48514	7884.8	2088.7	12672

TABLE 11 Summary of robust designs identified by regret analysis.

Criterion	WWR (%)	Rotation (°)	Façade configuration	Plan ratio	Regret	Notes
Minimax regret (risk-averse)	40	45	Single	Type-2	0.059792	Limits loss in the worst climate
Average regret (risk-neutral)	60	0	Single	Type-1	0.033526	Minimises average loss across climates

Across all climates, CO_2 and energy values remained relatively stable, while discomfort showed greater variability. This confirms that the design performs consistently in terms of environmental impact, with comfort outcomes that are more sensitive to local conditions.

3.4.2 Regret-based evaluation

The regret analysis tested how far candidate designs deviated from the climate-optimal solution. Two robust archetypes were identified (Table 11):

- Minimax regret (risk-averse): WWR ≈40%, orientation ≈45°, Single façade, Type-2 plan ratio. This solution mitigated worst-case performance losses, achieving a maximum regret of 0.0598, even in the most unfavourable conditions.
- Average regret (risk-neutral): WWR ≈60%, orientation ≈0°, Single façade, Type-1 plan ratio. This solution achieved the lowest average regret (0.0335), staying close to local optima in most climates but with greater variability under extreme conditions.

The two approaches together highlight complementary robust strategies:

- The mean–variance candidate provided stable performance with relatively low dispersion across climates, performing best in Mediterranean and arid regions.
- The minimax regret solution ensured resilience in the worst-case scenarios, offering a conservative but reliable choice.
- The average regret solution aligned most closely with local optima across the majority of climates, resulting in higher efficiency in most cases.

Both criteria confirmed that the recommendations are applicable and robust across climates. The mean–variance approach identified a single design with consistently strong performance and low variability (Tables 9, 10). In contrast, the regret analysis distinguished between a minimax solution, which limits losses under the most adverse climate, and a risk-neutral solution, which minimises average loss (Table 11). Overall, robustness analysis confirms that while optimal designs differ by climate, a limited set of robust candidates can still deliver acceptable trade-offs across diverse contexts. These results bridge highly tailored climate strategies and globally resilient archetypes.

4 Discussion

This study examined the performance of library reading halls across 9 Köppen climate zones using exploratory data analysis, explainable machine learning, multi-objective optimisation, and robustness evaluation. The findings advance knowledge on climate-adaptive passive design, offering both precise design thresholds and cross-contextual strategies. Given the use of standardised assumptions and the absence of calibration with monitored library data, the results should be interpreted within a comparative framework. Specifically, the findings are intended to reveal relative trends, sensitivities, and cross-climatic contrasts under controlled modelling conditions, rather than to provide absolute predictions of energy use or comfort performance for any individual library building. Accordingly, the findings should be understood primarily as comparative indicators of design sensitivity and cross-climatic trends under controlled assumptions, rather than as absolute predictions of operational energy use or comfort levels for individual library buildings. The standardised modelling framework adopted in this study was

intentionally designed to support consistent cross-climatic comparison, at the expense of site-specific calibration, and therefore prioritises relative performance insights over absolute accuracy.

4.1 Climatic dependency and parameter hierarchy

The analysis confirmed that climate is the dominant determinant of building performance, with design parameters exerting secondary but still meaningful influences. This finding is consistent with earlier work emphasising climate as the primary driver of thermal comfort and energy demand (de Dear and Brager, 1998). WWR emerged as the most influential design lever within this climatic envelope, corroborating studies that link glazing ratio to energy demand and daylight availability (Goia, 2016; Yeom et al., 2020). Significantly, this study advances prior research by quantifying cross-climatic thresholds: discomfort minima at 30%–40%, penalties below 13.6%, and steep inflection points at approximately 56.4% and 83.6%. Such precision provides actionable, climate-sensitive decision rules for library reading halls, where occupants spend long hours under stringent visual and thermal demands. Façade configuration ranked second, moderating glazing effects and shaping solar gain and ventilation potential, as highlighted in prior work on shading and façade systems (Tzempelikos and Athienitis, 2007) and their implications for comfort (Frontczak and Wargocki, 2011).

The consistently superior performance of single façades across various climates suggests that envelope simplicity can enhance robustness, challenging the assumption that multi-layered façades always yield better efficiency (Carlucci et al., 2020). The orientation and plan ratios were less influential globally but became more important in specific contexts. In hot-arid zones, east–west orientations were penalised by solar asymmetry, a pattern consistent with findings showing directional differences in solar availability and exposure across urban fabrics (Compagnon, 2004). Plan ratio influenced performance through surface-to-volume relationships and daylight penetration, consistent with morphology–performance interactions reported in prior research (Okeil, 2010) (Susorova et al., 2013). Overall, the SHAP analysis delineates a consistent hierarchy of determinants, climate, WWR, façade configuration, and orientation/plan ratio, that can guide the prioritisation of early-stage design decisions.

Accordingly, the findings should be interpreted at the climate-class level, with individual cities serving only as illustrative representatives of broader Köppen–Geiger categories. The results, therefore, provide climate-class-level guidance under standardised modelling assumptions, rather than city-specific or geographically bound design prescriptions.

4.2 Trade-offs and optimisation outcomes

The Pareto-based optimisation confirmed that comfort, energy, and CO_2 emissions cannot be minimised simultaneously, consistent with prior multi-objective optimisation research (Machairas et al., 2014; Nguyen et al., 2014). The contribution of this study lies in visualising these trade-offs across nine climates and identifying both global and climate-specific archetypes. Three global archetypes emerged from the optimisation:

- Comfort-focused archetype: substantially reduced discomfort hours but at the cost of higher energy use and emissions.
- Energy/CO_2-focused archetype: achieved the lowest emissions and energy demand but imposed significant comfort penalties.
- Balanced archetype: delivered moderate performance across all metrics, representing a compromise strategy.

Similar archetype-based frameworks have been observed in optimisation studies of offices and dwellings (Ascione et al., 2017b; Hamdy et al., 2011), but this study extends the approach to libraries, which are highly occupied, visually demanding spaces. The climate-specific archetypes highlight divergent pathways:

- Tropical climates varied between very low WWR values (reducing solar gains) and very high WWR values (enhancing daylight and ventilation).
- Arid and Mediterranean climates stabilised around moderate WWR bands, reflecting balanced solar exposure.
- Temperate climates showed broader distributions, consistent with seasonal variability in mixed conditions (Santamouris, 2016)
- Continental climates remained constrained by persistent discomfort due to long heating periods, even when energy and CO_2 remained moderate.

Taken together, these findings reinforce the notion that there is no universal optimum, and design strategies must be tailored to climatic realities (Shi et al., 2016; Kheiri, 2018).

The study's findings indicate a relationship between total energy consumption and CO_2 emissions. However, this does not imply that the two objectives are identical. In addition to the magnitude of energy use, CO_2 emissions also reflect the energy carriers through which this demand is supplied. In the DesignBuilder–EnergyPlus simulations, city-specific EPW climate files determine the relative distribution of heating and cooling loads, thereby altering the balance between natural gas for heating and electricity for cooling, as well as for auxiliary systems (including lighting and equipment). CO_2 emissions are calculated using fuel-specific emission factors defined within the EnergyPlus framework. As a result, even design solutions with similar total energy consumption levels may exhibit different CO_2 emission profiles due to climate-driven differences in fuel use. Within this context, CO_2 is treated not as an independent physical variable but as a policy-oriented environmental performance indicator representing the climate impact of energy demand. Although energy and CO_2 outputs are mathematically correlated under the adopted assumptions, they serve distinct interpretative roles within the optimisation framework. Accordingly, the methodological and analytical validity of the three-objective formulation (discomfort–energy–CO_2) is preserved. While it is well recognised that electricity grid carbon intensity varies by country and region, the use of location-specific grid emission factors would introduce additional supply-side variability and weaken the study's climate- and envelope-focused comparative structure. Therefore,

the adopted approach prioritises isolating the effects of climatic conditions and passive design parameters on building performance over differences in energy supply. Future research may extend the present framework by incorporating region-specific electricity grid carbon intensities and hybrid energy supply scenarios, enabling a more detailed decoupling of energy consumption and carbon emissions.

4.3 Robustness and cross-contextual design strategies

While optimisation identifies climate-specific optima, practice often requires robust solutions that perform reliably across diverse contexts. Robustness has gained recognition in building performance research as a necessary complement to optimisation, particularly under climatic uncertainty (Carlucci et al., 2015; Hopfe and Hensen, 2011; Tian et al., 2018; Lu et al., 2020). The mean–variance evaluation highlighted a mid-range configuration (WWR = 60%, orientation = 195°, Single façade, Type-2) that delivered balanced outcomes with relatively low variability across climates.

This finding reinforces the potential of intermediate glazing ratios and simple envelope configurations to provide stable performance under contrasting environmental conditions. It is noteworthy that the mathematically 'robust' solution (WWR 60%) exceeds the 'sweet spot' range (30%–40%) identified in the PDP analysis. This divergence occurs because the mean–variance criterion rewards the significant energy savings from larger windows in cloudy climates, balancing the thermal penalties. However, while WWR 60% is 'robust' in terms of total energy and carbon, it sits closer to the threshold of thermal and visual risk. Therefore, the 30%–40% range remains the 'safer' passive recommendation, whereas the 60% solution represents a high-performance alternative that is viable only with advanced shading integration.

The regret-based analysis was complemented by this, distinguishing between risk-averse and risk-neutral strategies (see Table 11). The minimax regret archetype limited worst-case losses, providing resilience under extreme or uncertain climates. In contrast, the average regret archetype achieved higher overall efficiency by keeping close to local optima across most climates, albeit at the cost of greater variability in outliers. These results show that although climate-specific optima diverge sharply, a limited set of archetypal strategies can serve as reliable baselines for decision-making under uncertainty. This positions robustness analysis as a practical bridge between highly tailored climate-sensitive designs and globally resilient approaches. Unlike traditional optimisation studies that rely on static 'best' solutions which may underperform under slight climatic deviations, the robustness framework presented here quantifies performance stability, offering a critical advantage for long-term building resilience against environmental uncertainty.

4.4 Implications for library design and operation

The findings have direct implications for the design of library reading halls, where prolonged stays and visual demands amplify the importance of both thermal and daylight comfort.

- Thermal–visual balance: While this study assessed discomfort thermally, elevated WWR increases the likelihood of glare and daylight saturation. When glazing ratios exceed ~40%, external shading, low-SHGC glazing, daylight-responsive dimming, and light shelves become essential. Therefore, designers should treat WWR recommendations above 40% as 'conditional optima' valid only if rigorous glare-control strategies are implemented to prevent visual discomfort (Tzempelikos and Athienitis, 2007).
- Envelope simplicity: Single façades consistently outperformed double façades, suggesting that simpler, well-insulated assemblies may deliver more predictable and robust outcomes than complex, multi-layered systems, consistent with earlier findings on the role of façade design in optimisation-oriented comfort and energy performance (Carlucci et al., 2015).
- Morphological strategies: Plan typology influenced comfort and energy differently: compact Type-1 forms reduced energy/CO_2, while Type-2 plans enhanced comfort. This underscores the role of morphological decision-making, which remains underexplored in library design research (Okeil, 2010; Susorova et al., 2013).
- Operational integration: Robust performance requires integrating passive decisions with active systems, including automated shading, daylight/CO_2 sensors, and demand-controlled ventilation. This aligns with studies highlighting the coupling of passive and active measures in educational buildings (Santamouris, 2016).

At a policy level, the results argue for climate-specific design guidelines with upper bounds on WWR, mandatory shading requirements for high-glazing scenarios, and the integration of multi-objective optimisation into procurement and early design competitions.

4.5 Methodological contributions

Methodologically, this study demonstrates the value of integrating surrogate modelling, explainable AI, and robustness evaluation within a unified framework for building design. Previous work has often applied optimisation to limited parameter sets (Machairas et al., 2014) or employed machine learning without transparent interpretability (Carlucci et al., 2020; Li et al., 2020). By combining XGBoost with SHAP, PDP, and Pareto analysis across nine climates, this research provides a transferable pipeline that produces both interpretable insights and robust optimisation outcomes.

The robustness analysis further advances methodological practice by operationalising risk-averse (minimax) and risk-neutral (average) regret strategies, offering practitioners systematic tools for decision-making under site- and climate-uncertainty. This integration of predictive accuracy, interpretability, and resilience extends the state of the art and can be adapted to other building typologies and performance objectives.

4.6 Limitations and future research

This study has several limitations that should be acknowledged. Visual comfort was controlled by a minimum threshold, while the

analysis primarily focused on thermal comfort. While this approach ensured sufficient illuminance, it did not explicitly optimise for glare (e.g., DGP). Consequently, high-WWR solutions (>60%) prioritise energy efficiency and implicitly assume the presence of adaptive shading to mitigate potential visual discomfort.

The comfort metric was restricted to thermal discomfort hours defined by the adaptive model and the 80% acceptability band (EN 16798-1/ASHRAE 55). While this user-centred, hour-based metric aligns with widely used overheating/underheating assessments, it does not capture other dimensions of comfort. This scoping reflects a deliberate distinction between static architectural definitions and dynamic operational controls. The study optimises the fixed envelope parameters, specifically geometric proportions and aperture ratios, that establish the building's fundamental passive potential. Glare is therefore treated as a transient, operational issue to be addressed through adaptive elements (e.g., internal blinds or dynamic shading) during detailed design stages, rather than constraining primary massing and fenestration decisions.

Moreover, the assumptions of sedentary occupancy and seasonal clothing (0.9 met; 0.50 clo in summer, 1.00 clo in winter; DesignBuilder/EnergyPlus "All Clothing") may not accurately reflect cultural attire and activity patterns across all regions. Uniform assumptions regarding metabolic rate (0.9 met), clothing insulation (0.5/1.0 clo), and occupancy schedules were applied across all climate zones. This choice was intentional and aligned with the study's primary objective: enabling a controlled cross-climate comparison of passive design sensitivities rather than replicating region-specific behavioural patterns. While cultural attire, activity levels, and adaptive behaviours (such as window operation or blind adjustment) are known to vary across regions, introducing climate-specific behavioural assumptions would confound climatic effects with socio-cultural variability. By holding occupant-related parameters constant, the analysis isolates the influence of climate and envelope design parameters on thermal comfort outcomes, ensuring comparability across Köppen–Geiger climate classes. Consequently, the reported discomfort hours should be interpreted as relative indicators of climatic sensitivity under standardised occupant conditions, rather than predictions of absolute comfort performance for specific populations. From a methodological perspective, changes in clothing insulation or metabolic rate would primarily shift the absolute magnitude of discomfort hours within each climate zone, and are unlikely to overturn the comparative climate-driven trends identified in this study. Future work could extend the present framework by incorporating region-specific behavioural scenarios and by triangulating thermal comfort through sensitivity analyses of clothing and activity levels, combined with complementary indices (e.g., PMV/PPD or SET*) and, where feasible, subjective POE data.

Visual comfort was indirectly considered in this study through lighting energy penalties; however, direct daylight quality metrics such as glare probability and spatial daylight distribution were not explicitly modelled. In library reading spaces, visual comfort factors, including glare control, uniformity, and daylight quality play a critical role in user satisfaction and reading performance. The present focus on energy, thermal comfort, and CO_2 performance was therefore a deliberate methodological choice aimed at maintaining tractability across a large parametric design space. Future research should extend the proposed framework by integrating explicit visual comfort indicators (e.g., UDI, DA, DGP/DGI) alongside thermal and energy objectives. In addition, future studies should incorporate acoustic and indoor air quality metrics, which are particularly critical in library reading environments, enabling a more holistic, user-centred assessment of passive design strategies.

The analysis was limited to four design parameters; additional variables, including shading devices, glazing types, insulation levels, and natural ventilation strategies, should be examined to capture a broader range of passive interventions. Plan ratios and façade configurations were restricted to simplified archetypes (1:1–1:2; single- vs. double-sided glazing). While this enabled tractable cross-comparison, it does not encompass the full variety of library designs, such as deeper plans, atria, or mixed-mode layouts. The models also assumed standardised occupancy and operational profiles, which provided a robust comparative baseline but inevitably excluded region-specific practices. Incorporating adaptive comfort models and conducting sensitivity analyses using alternative behavioural profiles would improve realism and strengthen transferability.

In keeping with this early-stage focus, the study excluded additional measures, such as external shading devices, glazing properties, insulation levels, and natural ventilation strategies, to preserve computational tractability and isolate geometry-driven envelope effects. Nevertheless, each of these measures may exert secondary yet significant influences on energy and comfort performance, particularly in high-glazing scenarios. Glazing properties and insulation levels can alter the balance of heat gains and losses at elevated WWRs, while natural ventilation strategies may attenuate cooling loads in hot and mixed climates, thereby moderating the apparent impact of WWR. Excluding shading devices is particularly critical for interpreting the identified WWR thresholds in high-solar climates. In such contexts, fixed or adaptive shading systems (e.g., horizontal overhangs or vertical louvres) are expected to substantially mitigate solar gains and glare risks associated with higher glazing ratios. Accordingly, the upper WWR thresholds reported in this study should be interpreted as conservative bounds under unshaded conditions, reflecting geometry-driven constraints rather than fully optimised façade solutions. Future studies that explicitly parameterise shading devices, glazing properties, and ventilation strategies may demonstrate an upward shift in acceptable WWR ranges in high-solar climates; however, such potential gains should be evaluated alongside the increased design and operational complexity they entail.

The models were not calibrated with monitored data from actual libraries in each climatic zone. This deliberate choice of standardisation enabled controlled cross-comparison but limits the interpretation of results as absolute performance predictions. Future research should therefore extend the framework through calibration with empirical datasets from representative libraries across different regions, and by incorporating sensitivity analyses of alternative operational profiles.

Robustness was assessed only under present climatic conditions. Extending the analysis to projected climate change scenarios is essential, as shifts in temperature and solar patterns could alter performance thresholds and parameter hierarchies

(IPCC, 2021). In addition, while explainable machine learning identified parameter sensitivities across climates, coupling this approach with calibrated datasets would further enhance interpretability and strengthen the transferability of findings to real-world design practice.

While international standards (e.g., IFLA, ASHRAE) were used to define occupancy and geometric baselines, actual library designs are shaped by region-specific cultural, social, and functional factors that extend beyond energy and environmental considerations. These differences were not represented in the present archetypal framework and should be addressed in future work through calibration with local case studies and inclusion of broader cultural and operational contexts. Addressing these limitations will not only extend the applicability of the findings but also support the development of climate-resilient and user-centred libraries.

4.7 Conclusion and recommendations

This study demonstrates the dual necessity of climate-specific optimisation and robust cross-contextual strategies in the design of library reading halls. The research quantified critical parameter thresholds, visualised multi-objective trade-offs, and operationalised risk-aware design strategies by integrating surrogate modelling, explainable AI, and robustness analysis. The findings show that while climate is the primary determinant of performance, design parameters such as WWR, façade configuration, orientation, and plan ratio can significantly shape outcomes within the same climatic context. This underscores the importance of moving beyond generic guidelines toward climate-sensitive, data-driven decision rules for practice. For research, it sets a methodological precedent for applying explainable AI and robustness frameworks to other educational building typologies.

From these findings, several actionable recommendations can be drawn:

1. Climate as baseline: Climate remains the dominant determinant, but WWR and façade configuration introduce substantial variation within the same climate zone.
2. Energy–comfort trade-offs: Energy use and CO_2 emissions generally align, enabling joint management, while discomfort remains more sensitive to climate and design parameters.
3. Critical thresholds: Actionable design rules include WWR in the 30%–40% range as a balance point, penalties below 13.6% and above 56%–84%, and orientation knees at 42°, 153°, 192°, 258°, and 342°.
4. Archetypes and robustness: Climate-specific archetypes provide localised guidance, but robust solutions identified by mean–variance and regret analysis offer resilience for projects under climatic uncertainty or multi-site portfolios.
5. Library-specific strategies: A mid-range WWR combined with Single façades and compact or Type-2 plans represents the most stable strategy across various climates.
6. Policy implications: Climate-specific regulations should include upper WWR limits, mandatory shading provisions for high-glazing scenarios, and requirements for early-stage multi-objective optimisation in public library projects.

5 Conclusion

Libraries present unique design challenges, requiring the reconciliation of long-duration thermal comfort with stringent energy targets and daylight access. This study advances practice-oriented guidance and methodological innovation by integrating exploratory data analysis, explainable machine learning, multi-objective optimisation, and robustness evaluation across 9 Köppen climate zones.

The findings demonstrate that envelope simplicity, mid-range glazing ratios, and strategically configured morphological strategies yield stable performance across climates, particularly when complemented by external shading and daylight-responsive controls. These insights provide designers with climate-sensitive guidelines that extend beyond prescriptive approaches, supporting informed decision-making at the earliest stages. At the policy level, the results highlight the importance of climate-specific regulatory frameworks, including enforceable upper bounds on WWR, mandatory shading for high-glazing scenarios, and the integration of multi-objective optimisation into procurement and competition processes. Formalising such measures in regulatory practice would facilitate the systematic incorporation of resilience and sustainability into future library projects.

Beyond design guidance and policy implications, the study advances methodological practice by integrating surrogate modelling with SHAP-based interpretability, partial dependence thresholds, and robustness metrics into a coherent analytical framework. This approach operationalises risk-aware design strategies that focus on comparative performance stability rather than static predictions, making them both transparent and generalisable. Extending this methodological pipeline to incorporate visual comfort indices, behavioural models, and future climate scenarios would further strengthen its applicability, ensuring that educational environments remain user-centred and climate-resilient under evolving conditions.

Taken together, these contributions establish a benchmark for climate-adaptive, AI-supported passive design research. While grounded in the library context, the framework and insights developed here offer a transferable pathway for balancing comfort, energy, and emissions across diverse educational typologies. By uniting predictive modelling, interpretability, and robustness, the study not only advances the research frontier but also provides a foundation for shaping future professional standards in resilient and sustainable architecture.

Data availability statement

The raw data supporting the conclusions of this article will be made available by the authors, without undue reservation.

Author contributions

GI: Conceptualization, Data curation, Formal Analysis, Funding acquisition, Investigation, Methodology, Project

administration, Resources, Software, Supervision, Validation, Visualization, Writing – original draft, Writing – review and editing. GÖ: Conceptualization, Data curation, Formal Analysis, Funding acquisition, Investigation, Methodology, Project administration, Resources, Software, Validation, Visualization, Writing – original draft.

Funding

The author(s) declared that financial support was not received for this work and/or its publication.

Conflict of interest

The author(s) declared that this work was conducted in the absence of any commercial or financial relationships that could be construed as a potential conflict of interest.

Generative AI statement

The author(s) declared that generative AI was not used in the creation of this manuscript.

Any alternative text (alt text) provided alongside figures in this article has been generated by Frontiers with the support of artificial intelligence and reasonable efforts have been made to ensure accuracy, including review by the authors wherever possible. If you identify any issues, please contact us.

Publisher's note

All claims expressed in this article are solely those of the authors and do not necessarily represent those of their affiliated organizations, or those of the publisher, the editors and the reviewers. Any product that may be evaluated in this article, or claim that may be made by its manufacturer, is not guaranteed or endorsed by the publisher.

References

Aflaki, A., Esfandiari, M., and Jarrahi, A. (2023). Multi-criteria evaluation of a library's indoor environmental quality in the tropics. *Buildings* 13 (5), 1233. doi:10.3390/buildings13051233

Aissi, H., Bazgan, C., and Vanderpooten, D. (2009). Min–max and min–max regret versions of combinatorial optimization problems: a survey. *Eur. J. Oper. Res.* 197 (2), 427–438. doi:10.1016/j.ejor.2008.09.012

AlAnzi, A., Seo, D., and Krarti, M. (2009). Impact of building shape on thermal performance of office buildings in Kuwait. *Energy Convers. Manag.* 50 (3), 822–828. doi:10.1016/j.enconman.2008.09.033

ANSI and ASHRAE (2022). *Ventilation for acceptable indoor air quality*, 2022. Washington, DC: American National Standards Institute (ANSI); Peachtree Corners, GA: ASHRAE Stand, 1–90.

Applegate, R. (2009). The library is for studying. Student preferences for study space. *J. Acad. Librariansh.* 35 (4), 341–346. doi:10.1016/j.acalib.2009.04.004

Ascione, F., Bianco, N., De Masi, R. F., Mauro, G. M., and Vanoli, G. P. (2017a). Energy retrofit of educational buildings: transient energy simulations, model calibration and multi-objective optimization towards nearly zero-energy performance. *Energy Build.* 144, 303–319. doi:10.1016/j.enbuild.2017.03.056

Ascione, F., Bianco, N., De Stasio, C., Mauro, G. M., and Vanoli, G. P. (2017b). Artificial neural networks to predict energy performance and retrofit scenarios for any member of a building category: a novel approach. *Energy* 118, 999–1017. doi:10.1016/j.energy.2016.10.126

ASHRAE (2020a). *ANSI/ASHRAE standard 55-2020*. Atlanta, GA: Thermal Environmental Conditions for Human Occupancy.

ASHRAE (2020b). *Standard method of test for the evaluation of building energy analysis computer programs*. Peachtree Corners, GA: ASHRAE.

Baba, A., Shahrour, I., and Baba, M. (2024). Indoor environmental quality for comfort learning environments: case study of Palestinian school buildings. *Buildings* 14 (5), 1296. doi:10.3390/buildings14051296

Banbury, S. P., and Berry, D. C. (2005). Office noise and employee concentration: identifying causes of disruption and potential improvements. *Ergonomics* 48 (1), 25–37. doi:10.1080/00140130412331311390

Ben-Tal, A., El Ghaoui, L., and Nemirovski, A. (2009). *Robust optimization*. Princeton University Press. doi:10.1515/9781400831050

Bertsimas, D., Brown, D. B., and Caramanis, C. (2011). Theory and applications of robust optimization. *SIAM Rev.* 53 (3), 464–501. doi:10.1137/080734510

Beyer, H.-G., and Sendhoff, B. (2007). Robust optimization – a comprehensive survey. *Comput. Methods Appl. Mech. Eng.* 196 (33), 3190–3218. doi:10.1016/j.cma.2007.03.003

BSI (2009). *EN 16798-1: energy performance of buildings - ventilation for buildings*. London: British Standards Institution (BSI). doi:10.3403/30297472u

Carlucci, S., Causone, F., De Rosa, F., and Pagliano, L. (2015). A review of indices for assessing visual comfort with a view to their use in optimization processes to support building integrated design. *Renew. Sustain. Energy Rev.* 47, 1016–1033. doi:10.1016/j.rser.2015.03.062

Carlucci, S., De Simone, M., Firth, S. K., Kjærgaard, M. B., Markovic, R., Rahaman, M. S., et al. (2020). Modeling occupant behavior in buildings. *Build. Environ.* 174, 1–53. doi:10.1016/j.buildenv.2020.106768

Chai, T., and Draxler, R. R. (2014). Root mean square error (RMSE) or mean absolute error (MAE)? – arguments against avoiding RMSE in the literature. *Geosci. Model Dev.* 7 (3), 1247–1250. doi:10.5194/gmd-7-1247-2014

Chen, L.-P. (2021). Practical statistics for data scientists: 50+ essential concepts using R and python. *Technometrics* 63 (2), 272–273. doi:10.1080/00401706.2021.1904738

Chen, T., and Guestrin, C. (2016). XGBoost: a scalable tree boosting system. *Proc. ACM SIGKDD Int. Conf. Knowl. Discov. Data Min.* 13-17-Augu, 785–794. doi:10.1145/2939672.2939785

CIBSE (2013). *TM52: the limits of thermal comfort: avoiding overheating*. London.

CIBSE (2015). Lighting Guide LG5: lighting for education.

CIBSE (2017). *TM59: design methodology for the assessment of overheating risk in homes*. London.

Coakley, D., Raftery, P., and Molloy, P. (2012). "Calibration of whole building energy simulation models: detailed case study of a naturally ventilated building using hourly measured data," in *Proc. 1st building simulation and optimization conf. (BSO12)*, 57–64.

Coello Coello, C. A. (2006). Evolutionary multi-objective optimization: a historical view of the field. *IEEE Comput. Intell. Mag.* 1 (1), 28–36. doi:10.1109/mci.2006.1597059

Compagnon, R. (2004). Solar and daylight availability in the urban fabric. *Energy Build.* 36 (4), 321–328. doi:10.1016/j.enbuild.2004.01.009

Crawley, D. B., Hand, J. W., Kummert, M., and Griffith, B. T. (2008). Contrasting the capabilities of building energy performance simulation programs. *Build. Environ.* 43 (4), 661–673. doi:10.1016/j.buildenv.2006.10.027

de Dear, R. J., and Brager, G. S. (1998). Developing an adaptive model of thermal comfort and preference. *ASHRAE Trans.* 104, 145–167.

Deb, K. (2001). Nonlinear goal programming using multi-objective genetic algorithms. *J. Oper. Res. Soc.* 52 (3), 291–302. doi:10.1057/palgrave.jors.2601089

Deb, K., and Gupta, H. (2005). "Searching for robust pareto-optimal solutions in multi-objective optimization," in *Lecture notes in computer science*. Berlin Heidelberg: Springer, 150–164. doi:10.1007/978-3-540-31880-4_11

Deb, K., Pratap, A., Agarwal, S., and Meyarivan, T. (2002). A fast and elitist multiobjective genetic algorithm: NSGA-II. *IEEE Trans. Evol. Comput.* 6 (2), 182–197. doi:10.1109/4235.996017

Department for Education and Skills (2004). *Briefing framework for secondary school projects. Revision of BB82: area guidelines for schools (secondary section)*. London: Department for Education and Skills, 1–66.

Du, X., Liu, X., Gao, F., and Zhou, Z. (2025). Energy saving and low carbon oriented renovation framework for educational buildings with Tianjin University case study. *Sci. Rep.* 15 (1), 28822. doi:10.1038/s41598-025-14687-5

Friedman, J. H. (2001). Greedy function approximation: a gradient boosting machine. *Ann. Stat.* 29 (5), 1189–1232. doi:10.1214/aos/1013203451

Frontczak, M., and Wargocki, P. (2011). Literature survey on how different factors influence human comfort in indoor environments. *Build. Environ.* 46 (4), 922–937. doi:10.1016/j.buildenv.2010.10.021

Goia, F. (2016). The optimal window-to-wall ratio in office buildings in different European climates and the implications on total energy saving potential. *Sol. Energy* 132, 467–492. doi:10.1016/j.solener.2016.03.031

Hamdy, M., Hasan, A., and Siren, K. (2011). Applying a multi-objective optimization approach for Design of low-emission cost-effective dwellings. *Build. Environ.* 46 (1), 109–123. doi:10.1016/j.buildenv.2010.07.006

Henninger, R. H., and Witte, M. J. (2004). *'EnergyPlus testing with ANSI/ASHRAE standard 140-2001 (BESTEST)'*, ernest Orlando lawrence Berkeley natl. Lab.

Hopfe, C. J. (2009). Uncertainty and sensitivity analysis in building performance simulation for decision support and design optimization.

Hopfe, C. J., and Hensen, J. L. M. (2011). Uncertainty analysis in building performance simulation for design support. *Energy Build.* 43 (10), 2798–2805. doi:10.1016/j.enbuild.2011.06.034

Hu, M., Zhang, K., Nguyen, Q., and Tasdizen, T. (2023). The effects of passive design on indoor thermal comfort and energy savings for residential buildings in hot climates: a systematic review. *Urban Clim.* 49, 101466. doi:10.1016/j.uclim.2023.101466

IESNA (2012). *The lighting handbook: reference and application*. 10th ed. New York: Illuminating Engineering Society of North America.

IPCC (2021). Climate change 2021 – the physical science basis.

ISO (2005). *ISO 7730: ergonomics of the thermal environment: analytical determination and interpretation of thermal comfort using calculation of the PMV and PPD indices and local thermal comfort criteria*. Geneva.

Izmir Tunahan, G., Altamirano, H., Unwin, J., and Ticleanu, C. (2022). Evaluation of daylight perception assessment methods. *Front. Psychol.* 13, 805796. doi:10.3389/fpsyg.2022.805796

Kheiri, F. (2018). A review on optimization methods applied in energy-efficient building geometry and envelope design. *Renew. Sustain. Energy Rev.* 92, 897–920. doi:10.1016/j.rser.2018.04.080

Kottek, M., Grieser, J., Beck, C., Rudolf, B., and Rubel, F. (2006). World Map of the Köppen-Geiger climate classification updated. *Meteorol. Z.* 15 (3), 259–263. doi:10.1127/0941-2948/2006/0130

Kouvelis, P., and Yu, G. (1997). "A Robust discrete optimization framework," in *Nonconvex optimization and its applications*. Springer US, 26–73. doi:10.1007/978-1-4757-2620-6_2

Latimer, K., and Niegaard, H. (2007). *IFLA library building guidelines: developments & reflections*. Berlin, New York: K. G. Saur. doi:10.1515/9783598440373

Li, S., Liu, L., and Peng, C. (2020). A review of performance-oriented architectural design and optimization in the context of sustainability: dividends and challenges. *Sustainability* 12 (4), 1427. doi:10.3390/su12041427

Lortie, C. (2017). R for data science. *J. Stat. Softw. (Book Review)* 77 (1), 1–3. doi:10.18637/jss.v077.b01

Lu, S., Li, J., and Lin, B. (2020). Reliability analysis of an energy-based form optimization of office buildings under uncertainties in envelope and occupant parameters. *Energy Build.* 209, 109707. doi:10.1016/j.enbuild.2019.109707

Lundberg, S. M., and Lee, S. I. (2017). A unified approach to interpreting model predictions. *Adv. Neural Inf. Process. Syst.* 2017-Decem (2), 4766–4775. doi:10.48550/arXiv.1705.07874

Lundberg, S. M., Erion, G., Chen, H., DeGrave, A., Prutkin, J. M., Nair, B., et al. (2020). From local explanations to global understanding with explainable AI for trees. *Nat. Mach. Intell.* 2 (1), 56–67. doi:10.1038/s42256-019-0138-9

Machairas, V., Tsangrassoulis, A., and Axarli, K. (2014). Algorithms for optimization of building design: a review. *Renew. Sustain. Energy Rev.* 31, 101–112. doi:10.1016/j.rser.2013.11.036

Markowitz, H. (1952). Portfolio selection. *J. Finance* 7 (1), 77. doi:10.2307/2975974

Nguyen, A.-T., Reiter, S., and Rigo, P. (2014). A review on simulation-based optimization methods applied to building performance analysis. *Appl. Energy* 113, 1043–1058. doi:10.1016/j.apenergy.2013.08.061

Nicol, J. F., and Humphreys, M. A. (2002). Adaptive thermal comfort and sustainable thermal standards for buildings. *Energy Build.* 34 (6), 563–572. doi:10.1016/S0378-7788(02)00006-3

Ochoa, C. E., Aries, M. B. C., and Hensen, J. L. M. (2012a). State of the art in lighting simulation for building science: a literature review. *J. Build. Perform. Simul.* 5 (4), 209–233. doi:10.1080/19401493.2011.558211

Ochoa, C. E., Aries, M. B. C., van Loenen, E. J., and Hensen, J. L. M. (2012b). Considerations on design optimization criteria for windows providing low energy consumption and high visual comfort. *Appl. Energy* 95, 238–245. doi:10.1016/j.apenergy.2012.02.042

Okeil, A. (2010). A holistic approach to energy efficient building forms. *Energy Build.* 42 (9), 1437–1444. doi:10.1016/j.enbuild.2010.03.013

Peel, M. C., Finlayson, B. L., and McMahon, T. A. (2007). Updated world map of the Köppen-Geiger climate classification. *Hydrol. Earth Syst. Sci.* 11 (5), 1633–1644. doi:10.5194/hess-11-1633-2007

Pellerin, N., and Candas, V. (2003). Combined effects of temperature and noise on human discomfort. *Physiol. Behav.* 78 (1), 99–106. doi:10.1016/s0031-9384(02)00956-3

Ratti, C., Baker, N., and Steemers, K. (2005). Energy consumption and urban texture. *Energy Build.* 37 (7), 762–776. doi:10.1016/j.enbuild.2004.10.010

Santamouris, M. (2016). Cooling the buildings – past, present and future. *Energy Build.* 128, 617–638. doi:10.1016/j.enbuild.2016.07.034

Savage, L. J. (1954). *The foundations of statistics*. John Wiley and Sons, Inc., 294. doi:10.1002/nav.3800010316

Sayadi, S., Hayati, A., and Salmanzadeh, M. (2021). Optimization of window-to-wall ratio for buildings located in different climates: an IDA-Indoor climate and energy simulation study. *Energies* 14 (7), 1974. doi:10.3390/en14071974

Shi, X., Tian, Z., Chen, W., Si, B., and Jin, X. (2016). A review on building energy efficient design optimization from the perspective of architects. *Renew. Sustain. Energy Rev.* 65, 872–884. doi:10.1016/j.rser.2016.07.050

Shwartz-Ziv, R., and Armon, A. (2022). Tabular data: deep learning is not all you need. *Inf. Fusion* 81, 84–90. doi:10.1016/j.inffus.2021.11.011

Silva, H. E., and Henriques, F. M. A. (2014). Microclimatic analysis of historic buildings: a new methodology for temperate climates. *Build. Environ.* 82, 381–387. doi:10.1016/j.buildenv.2014.09.005

Silva, H. E., and Henriques, F. M. A. (2015). Preventive conservation of historic buildings in temperate climates. The importance of a risk-based analysis on the decision-making process. *Energy Build.* 107, 26–36. doi:10.1016/j.enbuild.2015.07.067

Som, S., and Gregory, M. (2011). "Empirical validation of building energy simulation software: energyplus," in *Proc. Building Simulation 2011 (IBPSA)* (Sydney, Australia), 2941–2948.

Susorova, I., Tabibzadeh, M., Rahman, A., Clack, H. L., and Elnimeiri, M. (2013). The effect of geometry factors on fenestration energy performance and energy savings in office buildings. *Energy Build.* 57, 6–13. doi:10.1016/j.enbuild.2012.10.035

Tawfeeq, H., and Qaradaghi, A. M. A. (2024). Optimising window-to-wall ratio for enhanced energy efficiency and building intelligence in hot summer Mediterranean climates. *Sustainability* 16 (17), 7342. doi:10.3390/su16177342

Thneibat, M. (2024). Assessing the post-COVID interaction between indoor environmental quality and occupants within educational buildings: a structural equation modeling approach. *Build. Environ.* 255, 111422. doi:10.1016/j.buildenv.2024.111422

Tian, W., Heo, Y., de Wilde, P., Li, Z., Yan, D., Park, C. S., et al. (2018). A review of uncertainty analysis in building energy assessment. *Renew. Sustain. Energy Rev.* 93, 285–301. doi:10.1016/j.rser.2018.05.029

Tregenza and Wilson, (2011). *Daylighting: architecture and lighting design*. London: Routledge.

Tukey, J. W. (1977). Exploratory data analysis. *Psychometrika* 42 (4), 635–638. doi:10.1007/bf02295986

Tunahan, G. I., and Altamirano, H. (2022). Seating behaviour of students before and after the COVID-19 pandemic: findings from occupancy monitoring with PIR sensors at the UCL bartlett Library. *Int. J. Environ. Res. Public Health* 19 (20), 13255. doi:10.3390/IJERPH192013255

Tzempelikos, A., and Athienitis, A. K. (2007). The impact of shading design and control on building cooling and lighting demand. *Sol. Energy* 81 (3), 369–382. doi:10.1016/j.solener.2006.06.015

Xie, X., Ni, Y., and Zhang, T. (2025). Machine-Learning-Enhanced building performance-guided form optimization of high-rise office buildings in China's hot summer and warm Winter Zone—A case study of Guangzhou. *Sustainability* 17 (9), 4090. doi:10.3390/su17094090

Yaman, G. Ö. (2025). Determination of optimum passive design parameters for industrial buildings in different climate zones using an energy performance optimization model based on an Artificial Neural Network (ANN) and Particle Swarm Optimization (PSO). *Sustainability* 17 (6), 2357. doi:10.3390/su17062357

Yeom, S., Kim, H., Hong, T., and Lee, M. (2020). Determining the optimal window size of office buildings considering the workers' task performance and the building's energy consumption. *Build. Environ.* 177, 106872. doi:10.1016/j.buildenv.2020.106872

Yu, J., Yang, C., and Tian, L. (2008). Low-energy envelope design of residential building in hot summer and cold winter zone in China. *Energy Build.* 40 (8), 1536–1546. doi:10.1016/j.enbuild.2008.02.020

Zitzler, E., Laumanns, M., and Thiele, L. (2001). SPEA2: improving the strength Pareto evolutionary algorithm.